Ms. for *Organometallics* (ARTICLE)

Reactivity of Amidinatosilylenes and Amidinatogermylenes with [$PtMe_2(\eta^4$-cod)]: *cis*- versus *trans*-[$PtMe_2L_2$] Complexes and Cyclometalation Reactions

Javier A. Cabeza,[,a] José M. Fernández-Colinas,[a] Pablo García-Álvarez,*[,a]*
Laura González-Álvarez,[a] and Enrique Pérez-Carreño[b]

[a]Centro de Innovación en Química Avanzada (ORFEO-CINQA network), Departamento de Química Orgánica e Inorgánica, Universidad de Oviedo, 33071 Oviedo, Spain

[b]Departamento de Química Física y Analítica, Universidad de Oviedo, 33071 Oviedo, Spain

*E-mail: jac@uniovi.es (J.A.C.) and pga@uniovi.es (P.G.-A.)

ABSTRACT: The reactions of [$PtMe_2(\eta^4$-cod)] (cod = 1,5-cyclooctadiene) with two equivalents of the amidinatotetrylenes E(^{t}Bu$_2$bzam)X (^{t}Bu$_2$bzam = *N*,*N'*-bis(tertbutyl)benzamidinate. E = Si; X = Mes (**1**$_{\text{Si-Mes}}$), CH_2SiMe_3 (**1**$_{\text{Si-Tmsm}}$); E = Ge; X = Mes (**1**$_{\text{Ge-Mes}}$), CH_2SiMe_3 (**1**$_{\text{Ge-Tmsm}}$)] led to disubstituted derivatives of generic formula [$PtMe_2${E(^{t}Bu$_2$bzam)X}$_2$] (**2**$_{\text{E-X}}$) in which the ligand arrangement is *trans* for the silylenes (*trans*-**2**$_{\text{Si-Mes}}$ and *trans*-**2**$_{\text{Si-Tmsm}}$) but *cis* for the germylenes (*cis*-**2**$_{\text{Ge-Mes}}$ and *cis*-**2**$_{\text{Ge-Tmsm}}$). DFT calculations indicated that the different stereochemistry observed for complexes **2**$_{\text{E-X}}$, E = Si (*trans*) and Ge (*cis*), has a kinetic origin. Both mesityl derivatives *trans*-**2**$_{\text{Si-Mes}}$ and *cis*-**2**$_{\text{Ge-Mes}}$ reacted with one equivalent of [$H(OEt_2)_2$][BARF] (BARF = B{3,5-$(CF_3)_2C_6H_3$}$_4$) to give isostructural ionic complexes, [Pt{E(^{t}Bu$_2$bzam)$C_6H_2(CH_2)Me_2$}{E(^{t}Bu$_2$bzam)Mes}][BARF] (E = Si (**3**$_{\text{Si-Mes}}$), Ge (**3**$_{\text{Ge-Mes}}$)) in which a cationic 14-electron platinum(II) complex is stabilized by both a cyclometalated tetrylene and a non-cyclometalated tetrylene that has a mesityl methyl group agostically interacting with the platinum atom.

INTRODUCTION

Heavier tetrylenes (HTs), which are heavier carbene analogues, have been incorporated as ligands to transition metal complexes since the 70s.[1,2] In recent years, new generations of HTs, mostly silylenes and germylenes that are donor-stabilized by chelating fragments, have been recognized as very strong electron-donating groups[3] and as versatile and steering ligands for homogeneous catalysis, boosting the interest in the coordination chemistry of this kind of molecules. Among the plethora of currently known donor-stabilized HTs, amidinato-HTs are playing a predominant role,[1a,d,f,2] possibly because their electronic and steric characteristics can be easily and extensively tuned, including the synthesis of polydentate variants.

On the other hand, cyclometalated complexes (cyclometalation has been defined as a metal-mediated activation of a ligand C–H bond to form a metalacycle[4]) have been used for decades in organic transformations and catalysis (activation of unreactive C–H bonds, cross-coupling, transfer hydrogenation, dehydrogenation, etc.),[5] in bioorganometallic chemistry (anticancer agents, enzyme prototypes, etc.)[5e,f,6] and in materials' science (photophysical devices, such as OLEDs and solar cells, liquid crystals, sensors, etc.).[5b,e,f,k,7] In fact, cyclometalation processes are extensively represented for all important types of ligands (amines, imines, pyridines, phosphanes, N-heterocyclic carbenes, etc.). However, when considering HTs, few cyclometalated examples have been hitherto reported[8-10] and most of them involve amidinato-HTs.[9,10] This is surprising taking into account that HTs have been used as ligands for at least 50 years[11] and that the donor-stabilized generations of these ligands are very strong electron donors (the oxidative addition of C–H bonds is easier for electron-rich metal complexes).[4b,12] In this context, as part of our investigations on amidinato-HTs,[1d,10,13] we have recently reported that the reactivity of the silylene Si(^{t}Bu$_2$bzam)Mes (**1**$_{\mathbf{Si\text{-}Mes}}$) with different iridium precursors is notably different from that of the isostructural germylene Ge(^{t}Bu$_2$bzam)Mes (**1**$_{\mathbf{Ge\text{-}Mes}}$) (Scheme 1).[10] Thus, while the cyclometalation of **1**$_{\mathbf{Si\text{-}Mes}}$ (upon C–H bond activation of a mesityl methyl group) was found to be inevitable in its room temperature reactions with [Ir$_2$(μ-Cl)$_2$(η^4-cod)$_2$] (cod = 1,5-cyclooctadiene) and [Ir$_2$Cl$_2$(μ-Cl)$_2$(η^5-Cp*)$_2$] (Cp* = 1,2,3,4,5-pentamethylcyclopentadienyl) (formation of **A** and **C**, respectively, in Scheme 1),[10] the same reactions using **1**$_{\mathbf{Ge\text{-}Mes}}$ led to noncyclometalated derivatives (**B** and **D**, respectively, in Scheme 1) and only the thermolysis of **D** at 90 °C allowed the isolation of a cyclometalated reaction product (the germanium analogue of compound **C**).[10a] The stronger electron-donor capacity of silylenes,

compared to that of analogous germylenes,[3,14] seems to be the key factor responsible for this different reactivity.

Scheme 1. Previously Reported Room Temperature Reactions of $\mathbf{1}_{Si\text{-}Mes}$ and $\mathbf{1}_{Ge\text{-}Mes}$ with Iridium(I) and Iridium(III) Complexes.

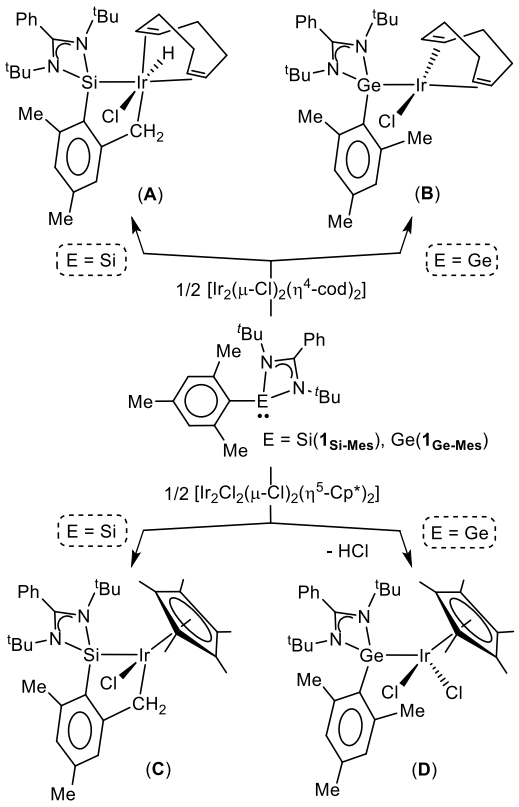

Aiming at further expanding the coordination chemistry of amidinato-HTs susceptible to participate in cyclometalation processes, we have now studied the reactivity of $[PtMe_2(\eta^4\text{-cod})]$ with two equivalents of E(*t*Bu$_2$bzam)X ($\mathbf{1_{E\text{-}X}}$) (E = Si, Ge; X = Mes, CH_2SiMe_3). These reactions, which are the first ones to combine HTs with $[PtMe_2(\eta^4\text{-cod})]$, did not render cyclometalated complexes at room temperature, but just led to square-planar bis(tetrylenes) derivatives of generic formula $[PtMe_2\{E(^t\text{Bu}_2\text{bzam})X\}_2]$ ($\mathbf{2_{E\text{-}X}}$). Remarkably, the stereochemistry of these reaction products has been found to be dictated not by the volume of the tetrylene ligands but by the nature of the tetrel atom, being *trans* for the silylenes (E = Si; $\mathbf{2_{Si\text{-}X}}$) but *cis* for the germylenes (E = Ge; $\mathbf{2_{Ge\text{-}X}}$). This surprising tetrel atom-dependence of the reaction stereoselectivity has been rationalized with the help of DFT calculations. Additionally, very interesting agostically-stabilized cyclometalated 14-electron platinum(II) cationic complexes have been prepared from reactions of the mesityl complexes *trans*-$\mathbf{2_{Si\text{-}Mes}}$ and *cis*-$\mathbf{2_{Ge\text{-}Mes}}$ with $[H(OEt_2)_2][BARF]$ (BARF = $B\{3,5\text{-}(CF_3)_2C_6H_3\}_4$).

RESULTS AND DISCUSSION

The amidinatotetrylenes $\mathbf{1}_{\mathbf{Si\text{-}Mes}}$ and $\mathbf{1}_{\mathbf{Ge\text{-}Mes}}$ (two equivalents) readily displaced the cod ligand of [$PtMe_2(\eta^4$-cod)] at room temperature to give *trans*-[$PtMe_2${Si(^{t}Bu$_2$bzam)Mes}$_2$] (*trans*-$\mathbf{2}_{\mathbf{Si\text{-}Mes}}$) and *cis*-[$PtMe_2${Ge(^{t}Bu$_2$bzam)Mes}$_2$] (*cis*-$\mathbf{2}_{\mathbf{Ge\text{-}Mes}}$), respectively (Scheme 2), as major reaction products (^{1}H NMR analysis of reaction solutions; Figure S17 of the Supporting Information), which were isolated as pure solids in good yields (79% and 62%, respectively).

Scheme 2. Reactions of [$PtMe_2(\eta^4$-cod)] with $\mathbf{1}_{\mathbf{E\text{-}X}}$

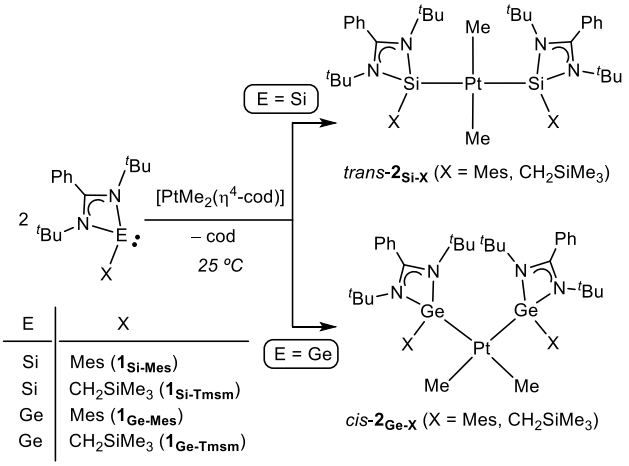

The X-ray diffraction (XRD) molecular structures of *trans*-$\mathbf{2}_{\mathbf{Si\text{-}Mes}}$ (Figure 1) and *cis*-$\mathbf{2}_{\mathbf{Ge\text{-}Mes}}$ (Figure 2) confirmed the square-planar coordination of the platinum atom and the presence of two methyl and two benzamidinato-HT ligands in each compound, but, while the ligand arrangement is *trans* in the silylene complex (Si1−Pt1−Si2 177.6(1)º), the germylene derivative features a *cis* stereochemistry (Ge1−Pt1−Ge2 106.82(4)º). Whilst the silylene ligands of *trans*-$\mathbf{2}_{\mathbf{Si\text{-}Mes}}$ present an approximate *syn* conformation around the Pt atom, the germylenes of *cis*-$\mathbf{2}_{\mathbf{Ge\text{-}Mes}}$ minimize their steric interactions being disposed in an approximate *anti* conformation. The Pt–Si (av. 2.317(5) Å; *trans*-$\mathbf{2}_{\mathbf{Si\text{-}Mes}}$) and Pt–Ge (av. 2.399(6) Å; *cis*-$\mathbf{2}_{\mathbf{Ge\text{-}Mes}}$) both lengths are over the top limit of the range of Pt–Si distances (2.208(2)–2.302(2) Å) and among the longest Pt–Ge distances (2.304(1)–2.409(1) Å) known for the few previously reported XRD-characterized platinum complexes equipped with terminal silylenes[15] and germylenes,[16] reflecting the large steric bulk of the $\mathbf{1}_{\mathbf{E\text{-}Mes}}$ ligands. The large size of the germylene ligands of *cis*-$\mathbf{2}_{\mathbf{Ge\text{-}Mes}}$ also accounts for the small C_{Me}–Pt–C_{Me} bond angle of *cis*-$\mathbf{2}_{\mathbf{Ge\text{-}Mes}}$ (av.[17] 84.5(2)°). The Pt–C_{Me} bond distances in *trans*-$\mathbf{2}_{\mathbf{Si\text{-}Mes}}$ (2.17(1) and 2.25(1) Å) and

are in the range known for $[PtMe_2L_2]$ (L = any ligand) complexes.[18] The methyl groups of *cis*-$\mathbf{2}_{\mathbf{Ge\text{-}Mes}}$ were found disordered in two positions,[17] preventing any bonding comparison.

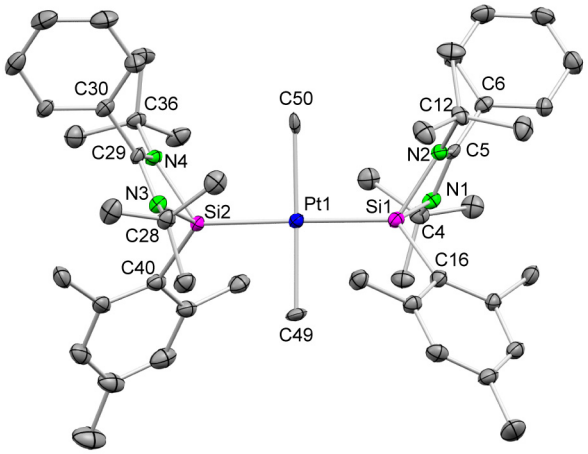

Figure 1. Molecular structure of *trans*-$\mathbf{2}_{\mathbf{Si\text{-}Mes}}$ (30% displacement ellipsoids, H atoms have been omitted for clarity). Selected bond lengths (Å) and angles (°): Pt1−C49 2.166(9), Pt1−C50 2.25(1), Pt1−Si1 2.321(2), Pt1−Si2 2.313(2), Si1−C16 1.918(8), Si1−N1 1.844(7), Si1−N2 1.864(6), N1−C4 1.487(9), N1−C5 1.34(1), N2−C5 1.34(1), N2−C12 1.489(9), C5−C6 1.48(1), Si2−C40 1.930(8), Si2−N3 1.859(7), Si2−N4 1.843(6), N3−C28 1.48(1), N4−C36 1.50(1), N3−C29 1.34(1), N4−C29 1.493(6), C29−C30 1.50(1); C49−Pt1−C50 177.1(5), Si1−Pt1−Si2 177.6(1), C49−Pt1−Si1 90.6(3), C49−Pt1−Si2 88.4(3), C50−Pt1−Si1 90.1(2), C50−Pt1−Si2 91.0(2), Pt1−Si1−N1 110.1(2), Pt1−Si1−N2 123.7(2), C16−Si1−Pt1 123.8(3), C16−Si1−N1 111.3(3), C16−Si1−N2 105.2(3), N1−Si1−N2 70.1(3), N1−C5−N2 105.6(6), Pt1−Si2−N3 110.5(2), Pt1−Si2−N4 122.8(2), C40−Si2−Pt1 125.6(3), C40−Si2−N3 110.7(4), C40−Si2−N4 103.7(3), N3−Si2−N4 70.2(3), N3−C29−N4 106.0(6).

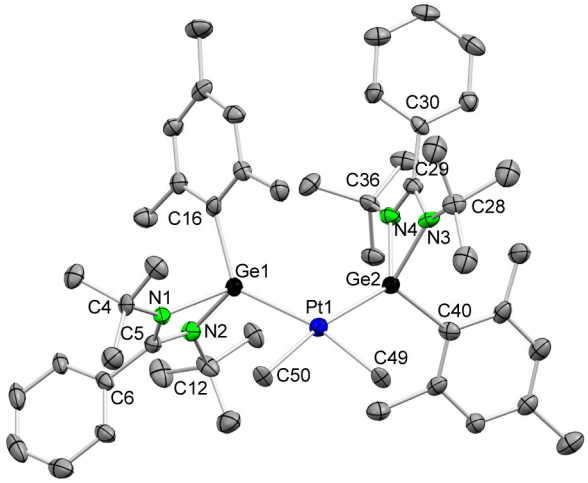

Figure 2. Molecular structure of *cis*-$\mathbf{2}_{\mathbf{Ge\text{-}Mes}}$ (30% displacement ellipsoids, H atoms have been omitted for clarity). Only one of the two positions in which the C28, C49 and C50 carbon atoms were found is shown. Selected bond lengths (Å) and angles (°), excluding those involving the disordered parts of the molecule: Pt1−Ge1 2.395(1), Pt1−Ge2 2.403(1), Ge1−C16 2.03(1), Ge1−N1 2.033(9), Ge1−N2 1.98(1), N1−C4 1.47(1), N1−C5 1.33(1), N2−C5 1.35(1), N2−C12 1.47(1), C5−C6 1.50(2), Ge2−C40 2.04(1), Ge2−N3 2.023(9), Ge2−N4 1.998(8), N3−C28 1.52(1), N4−C36 1.48(1), N3−C29 1.34(1), N4−C29 1.34(1), C29−C30 1.48(1); Ge1−Pt1−Ge2 106.82(4), Pt1−Ge1−N1 119.1(2), Pt1−Ge1−N2 115.6(3), C16−Ge1−Pt1 129.6(3), C16−Ge1−N1 99.3(4), C16−Ge1−N2 108.9(4), N1−Ge1−N2 66.1(3), N1−C5−N2 110(1), Pt1−Ge2−N3 116.4(2), Pt1−Ge2−N4 129.9(3), C40−Ge2−Pt1 121.4(3), C40−Ge2−N3 107.7(4), C40−Ge2−N4 102.3(4), N3−Ge2−N4 65.1(4), N3−C29−N4 107.9(9).

Previous reports have shown that the size of the tetrel atom can have a decisive impact on the steric properties of isostructural HTs (the smaller the tetrel atom the greater the steric bulk of the HTs ligand).[13d,19] Therefore, we reasoned that the more sterically alleviated *trans* configuration of *trans*-$\mathbf{2}_{\mathbf{Si\text{-}Mes}}$, in comparison to the more congested *cis* disposition of *cis*-$\mathbf{2}_{\mathbf{Ge\text{-}Mes}}$, might be related to the greater steric hindrance exerted by the silylene $\mathbf{1}_{\mathbf{Si\text{-}Mes}}$. In fact, such a relationship has been described for the reactions of the first generation Grubbs' catalyst *trans*-[$RuCl_2(CHPh)(PCy_3)_2$] with the amidinatogermylenes Ge(^{t}Bu$_2$bzam)X (X = ^{t}Bu, CH_2SiMe_3), which led to disubstituted derivatives differing in the arrangement of their HTs, being *trans* for X = ^{t}Bu but *cis* for the smaller X group CH_2SiMe_3. Having these precedents in mind and aiming at gathering more information on the factors controlling the observed reaction stereoselectivity, [$PtMe_2(\eta^4$-cod)] was also treated at room temperature with two equivalents of the less sterically demanding tetrylenes $\mathbf{1}_{\mathbf{Si\text{-}Tmsm}}$ and $\mathbf{2}_{\mathbf{Ge\text{-}Tmsm}}$, featuring a CH_2SiMe_3 moiety instead of a Mes fragment attached to the tetrel atom. Remarkably, these smaller tetrylenes afforded *trans*-[$PtMe_2${Si(^{t}Bu$_2$bzam)CH_2SiMe_3}$_2$] (*trans*-$\mathbf{2}_{\mathbf{Si\text{-}Tmsm}}$) and *cis*-[$PtMe_2${Ge(^{t}Bu$_2$bzam)$CH_2SiMe_3$}$_2$] (*cis*-$\mathbf{2}_{\mathbf{Ge\text{-}Tmsm}}$) as major products (^{1}H NMR analysis; Figure S18 of the Supporting Information) of the corresponding reactions (Scheme 2). The high solubility of *trans*-$\mathbf{2}_{\mathbf{Si\text{-}Tmsm}}$ and *cis*-$\mathbf{2}_{\mathbf{Ge\text{-}Tmsm}}$ was responsible for their isolation in moderate yields as pure products (61% and 40%, respectively).

The stereochemistry of *trans*-$\mathbf{2}_{\mathbf{Si\text{-}Tmsm}}$ and *cis*-$\mathbf{2}_{\mathbf{Ge\text{-}Tmsm}}$ was unambiguously established by XRD (Figures 3 and 4). The germylene derivative *cis*-$\mathbf{2}_{\mathbf{Ge\text{-}Tmsm}}$ is structurally analogous to *cis*-$\mathbf{2}_{\mathbf{Ge\text{-}Mes}}$, but *trans*-$\mathbf{2}_{\mathbf{Si\text{-}Tmsm}}$, while maintaining the same *trans* ligand arrangement as that of *trans*-$\mathbf{2}_{\mathbf{Si\text{-}Mes}}$, it displays a perfect *anti* conformation of the silylene ligands, resulting in a centrosymmetric structure. The Pt–Si and Pt–Ge bonds of *trans*-$\mathbf{2}_{\mathbf{Si\text{-}Tmsm}}$ (2.297(1) Å) and *cis*-$\mathbf{2}_{\mathbf{Ge\text{-}Tmsm}}$ (av. 2.368(5) Å) are *ca*. 0.02 Å and 0.03 Å shorter than those found for *trans*-$\mathbf{2}_{\mathbf{Si\text{-}Mes}}$ and *cis*-$\mathbf{2}_{\mathbf{Ge\text{-}Mes}}$, respectively, reflecting the smaller size of $\mathbf{1}_{\mathbf{E\text{-}Tmsm}}$. The Pt–$C_{Me}$ bond distances are nearly identical in both complexes (2.131(5) Å in *trans*-$\mathbf{2}_{\mathbf{Si\text{-}Tmsm}}$ and av. 2.12(1) Å in *cis*-$\mathbf{2}_{\mathbf{Ge\text{-}Tmsm}}$).

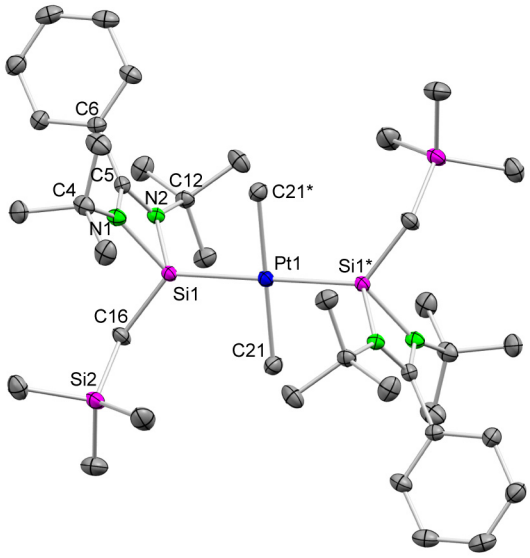

Figure 3. Molecular structure of *trans*-**2**$_{\text{Si-Tmsm}}$ (30% displacement ellipsoids, H atoms have been omitted for clarity). Selected bond lengths (Å) and angles (°): Pt1−C21 2.131(5), Pt1−Si1 2.297(1), Si1−C16 1.890(5), Si1−N1 1.863(4), Si1−N2 1.861(4), N1−C4 1.483(6), N1−C5 1.324(7), N2−C5 1.337(6), N2−C12 1.473(6), C5−C6 1.493(7); C21−Pt1−C21* 180.0(0), Si1−Pt1−Si1* 180.0(0), C21−Pt1−Si1 90.4(1), C21−Pt1−Si1* 89.6(1), Pt1−Si1−N1 122.5(1), Pt1−Si1−N2 113.6(1), C16−Si1−Pt1 127.2(2), C16−Si1−N1 105.4(2), C16−Si1−N2 102.1(2), N1−Si1−N2 70.0(2), N1−C5−N2 106.7(4).

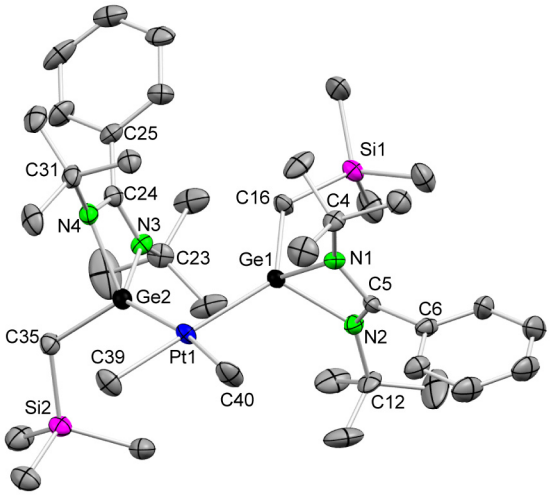

Figure 4. Molecular structure of *cis*-**2**$_{\text{Ge-Tmsm}}$ (25% displacement ellipsoids, H atoms have been omitted for clarity). Only one of the two analogous independent molecules of the asymmetric unit is shown. Selected bond lengths (Å) and angles (°): Pt1−C39 2.13(1), Pt1−C40 2.11(1), Pt1−Ge1 2.371(1), Pt1−Ge2 2.364(1), Ge1−C16 1.98(1), Ge1−N1 2.00(1), Ge1−N2 1.98(1), N1−C4 1.46(1), N1−C5 1.33(2), N2−C5 1.31(2), N2−C12 1.49(1), C5−C6 1.52(2), Ge2−C35 1.99(1), Ge2−N3 2.02(1), Ge2−N4 1.995(9), N3−C23 1.46(1), N4−C31 1.48(2), N3−C24 1.34(12), N4−C24 1.34(2), C24−C25 1.47(2); C39−Pt1−C40 82.8(6), Ge1−Pt1−Ge2 99.08(4), C39−Pt1−Ge1 173.0(4), C39−Pt1−Ge2 87.0(4), C40−Pt1−Ge1 91.1(4), C40−Pt1−Ge2 169.8(4), Pt1−Ge1−N1 117.6(3), Pt1−Ge1−N2 118.1(3), C16−Ge1−Pt1 127.8(4), C16−Ge1−N1 102.2(4), C16−Ge1−N2 108.0(5), N1−Ge1−N2 66.0(4), N1−C5−N2 110(1), Pt1−Ge2−N3 130.0(3), Pt1−Ge2−N4 118.1(3), C35−Ge2−Pt1 124.6(4), C35−Ge2−N3 100.8(5), C35−Ge2−N4 100.8(5), N3−Ge2−N4 65.2(4), N3−C24−N4 108(1).

Regarding the solution structures, the NMR spectra of *trans*-$\mathbf{2}_{\mathbf{Si\text{-}Tmsm}}$ and *cis*-$\mathbf{2}_{\mathbf{Ge\text{-}X}}$ indicated equivalence of the two metal-bound methyl groups and also of both amidinato-HTs (one signal for the four N^{t}Bu groups, one set of signals for the two CH_2SiMe_3 groups of *trans*-$\mathbf{2}_{\mathbf{Si\text{-}Tmsm}}$ and *cis*-$\mathbf{2}_{\mathbf{Ge\text{-}Tmsm}}$, and one set of signals for the two Mes fragments of *cis*-$\mathbf{2}_{\mathbf{Ge\text{-}Mes}}$). Concerning *trans*-$\mathbf{2}_{\mathbf{Si\text{-}Mes}}$, the silylenes are inequivalent, since two singlets are observed in the $^{29}Si\{^1H\}$ NMR spectrum (δ 72.4 and 71.7 ppm) and two N*C*N signals in the $^{13}C\{^1H\}$ spectrum (δ 166.3 and 165.9 ppm), suggesting restricted rotation of the benzimidinatosilylene groups about the Pt–Si bonds. However, this inequivalence is not evident from the signals of the metal bound methyls [$\delta(^1H)$ = 1.01 ppm (m, 6 H); $\delta(^{13}C)$ = –16.9 ppm (s, sat, J_{Pt-C} = 217 Hz)] and of the N^{t}Bu groups [$\delta(^1H)$ = 1.36 ppm (s, 36 H); $\delta(^{13}C)$ = 54.1 (4 *C* of ^{t}Bu), 31.0 (12 *C*H$_3$ of ^{t}Bu].

Therefore, as the silylene complexes are *trans* whereas the germylene derivatives are *cis*, regardless of the steric bulk of their HT ligands, the stereoselectivity of the reactions of [$PtMe_2(\eta^4$-cod)] with $\mathbf{1}_{\mathbf{E\text{-}R}}$ seems to be dictated by the nature of the ligand tetrel atom. It is also worth mentioning that the *trans* stereoselectivity of the silylene complexes *trans*-$\mathbf{2}_{\mathbf{Si\text{-}X}}$ is very rare, since it is known that reactions of [$PtMe_2(\eta^4$-cod)] with two equivalents of phosphanes[20] or NHCs[21] of different steric bulk give exclusively *cis*-isomers upon cod displacement. In fact, the silylene derivatives *trans*-$\mathbf{2}_{\mathbf{Si\text{-}X}}$ are, as far as we are aware, the first crystallographically characterized *trans*-[$PtMe_2L_2$] (L = any ligand) complexes.[18]

In order to gain insights into this apparent tetrel-assisted reaction stereoselectivity, the structures of the *trans* and *cis* stereoisomers of [$PtMe_2\{E(^tBu_2bzam)X\}_2$] (X = Mes, CH_2SiMe_3; E = Si, Ge) (Figures S9-S16 of the Supporting Information) were optimized by DFT methods (at the wb97xd/cc-pVDZ/SDD(Pt) level of theory).[22] Surprisingly, this study indicated that the *trans* configuration is more stable for the complexes with X = Mes (*trans*-$\mathbf{2}_{\mathbf{Si\text{-}Mes}}$ and *trans*-$\mathbf{2}_{\mathbf{Ge\text{-}Mes}}$ are 4.9 and 1.5 kcal mol^{-1} more stable than *cis*-$\mathbf{2}_{\mathbf{Si\text{-}Mes}}$ and *cis*-$\mathbf{2}_{\mathbf{Ge\text{-}Mes}}$, respectively), whereas the *cis* arrangement is more stable for the complexes with X = CH_2SiMe_3 (*cis*-$\mathbf{2}_{\mathbf{Si\text{-}Tmsm}}$ and *cis*-$\mathbf{2}_{\mathbf{Ge\text{-}Tmsm}}$ are 2.3 and 3.1 kcal mol^{-1} more stable than *trans*-$\mathbf{2}_{\mathbf{Si\text{-}Tmsm}}$ and *trans*-$\mathbf{2}_{\mathbf{Ge\text{-}Tmsm}}$, respectively). As these data are strongly related to the size of the HT ligands (the Mes group is larger than the CH_2SiMe_3 group), they do not rationalize the experimental results. Therefore, the different stereochemistry observed for the complexes with E = Si (*trans*) *vs*. those with E = Ge (*cis*) must have a kinetic origin. To support this hypothesis, a DFT mechanistic study was carried out.

The progress of the mechanistic calculations of the processes leading to *cis- and trans*-[$PtMe_2$(**1**$_{E\text{-}Mes}$)$_2$] (E = Si, Ge) resulted unacceptably slow due to the large number of atoms of these systems. Therefore, considering that, given the large steric bulk of the ligands, the transformation of the monotetrylene intermediates *cis*-[$PtMe_2$(η^2-cod)(**1**$_{E\text{-}Mes}$)] into the *trans*-[$PtMe_2$(η^2-cod)(**1**$_{E\text{-}Mes}$)] isomers should take place prior to the entrance of the second **1**$_{E\text{-}Mes}$ ligand, we decided to reduce our mechanistic study to the formation of the monosilylene and monogermylene intermediates *cis*-[$PtMe_2$(η^2-cod)(**1**$_{E\text{-}Mes}$)] (E = Si, Ge)) from [$PtMe_2$(η^4-cod)] and one equivalent of **1**$_{E\text{-}Mes}$ (E = Si, Ge) and their subsequent isomerization to *trans*-[$PtMe_2$(η^2-cod)(**1**$_{E\text{-}Mes}$)]. In fact, Venkatesan *et al*. reported that the *cis* to *trans* isomerization of *cis*-[$Pt(CCPh)_2(dbim)_2$] (dbim = *N*,*N*'-didodecylbenzimidazolin-2-ylidene), which features two bulky NHC ligands, needs a temperature of 200 °C or, alternatively, 75 °C in the presence of catalytic amounts of [$Pt(CCR)_2$(η^4-cod)].[23] The energy profiles of both systems (E = Si, Ge) are shown in Figure 5 (it only shows the optimized structures of the stationary points of the silicon system). Initially, both starting reagents form an encounter complex (**ec1**; Si···Pt 4.743 Å, Ge···Pt 4.622 Å) that evolves, *via* transition state **ts1**, in which **1**$_{E\text{-}Mes}$ occupies the axial position of a square pyramidal ligand environment, to an intermediate (**i1**; Si–Pt 2.394 Å, Ge–Pt 2.516 Å) that has a methyl and one of the olefinic groups occupying the axial positions of a distorted trigonal bipyramidal ligand arrangement. Subsequently, intermediate **i1** undergoes an almost barrierless decoordination of one olefinic moiety to form the square planar intermediate *cis*-[$PtMe_2$(η^2-cod)(**1**$_{E\text{-}Mes}$)] (**i2**; Si–Pt 2.339 Å, Ge–Pt 2.421 Å). The formation of **i2** is exergonic for both systems ($\Delta G_{(i2)}$ = –9.5 (E = Si), –3.4 (E = Ge) kcal mol^{-1}) and is kinetically allowed at room temperature ($\Delta G_{(ts1)}$ = 16.9 (E = Si), 15.1 (E = Ge) kcal mol^{-1}). The slightly different relative energies of **i2**$_{Si}$ and **i2**$_{Ge}$, which only differ in the nature of the tetrel atom, are much more marked in the stationary points involved in their isomerization to *trans*-[$PtMe_2$(η^2-cod)(**1**$_{E\text{-}Mes}$)] (**i4**), a transformation that occurs in two steps. First, *via* a quasi decoordination-recoordination of the η^2-cod ligand (**ts3**), a *trans* isomer (**i3**) is formed, which undergoes an easy conformational reorganization of the η^2-cod to finally form **i4** (Si–Pt 2.281 Å, Ge–Pt 2.372 Å). Similar isomerizations of square planar platinum(II) complexes, consisting of ligand quasi dissociation (as in **ts3**) and recoordination leading to a *trans* complex are well known.[23] Interestingly, the *cis* to *trans* conversion has a lower energy barrier and is more exergonic for E = Si than for E = Ge ($\Delta G_{(ts3)}$ = 15.9 (E = Si), 23.4 (E = Ge) kcal mol^{-1}; $\Delta G_{(i4–i2)}$ = –4.5 (E = Si), –0.1 (E = Ge)) and a barrier of 23.4

kcal mol^{-1} (**ts3**$_{Ge}$) does not allow a room temperature isomerization (or makes it very slow). Thus, while the complete mechanism has not been elucidated, it seems that the different stereochemistry observed for **1**$_{Si\text{-}Mes}$ (*trans*) and **1**$_{Ge\text{-}Mes}$ (*cis*) possibly arises from the fact that the *cis* to *trans* isomerization of the monosubsituted intermediate [PtMe$_2$(η^2-cod)(**1**$_{E\text{-}Mes}$)] is kinetically and thermodynamically more favoured for E = Si than for E = Ge. The final room temperature substitution of the η^2-cod ligand by the second equivalent of the corresponding tetrylene **1**$_{E\text{-}Mes}$ seems to take place on **i4** in the case of E = Si (leading to *trans*-[PtMe$_2$(**1**$_{Si\text{-}Mes}$)$_2$]), but on **i2** in the case of E = Ge (leading to *cis*-[PtMe$_2$(**1**$_{Ge\text{-}Mes}$)$_2$]). A similar rationale can explain the results of the **1**$_{E\text{-}Tmsm}$ ligand system.

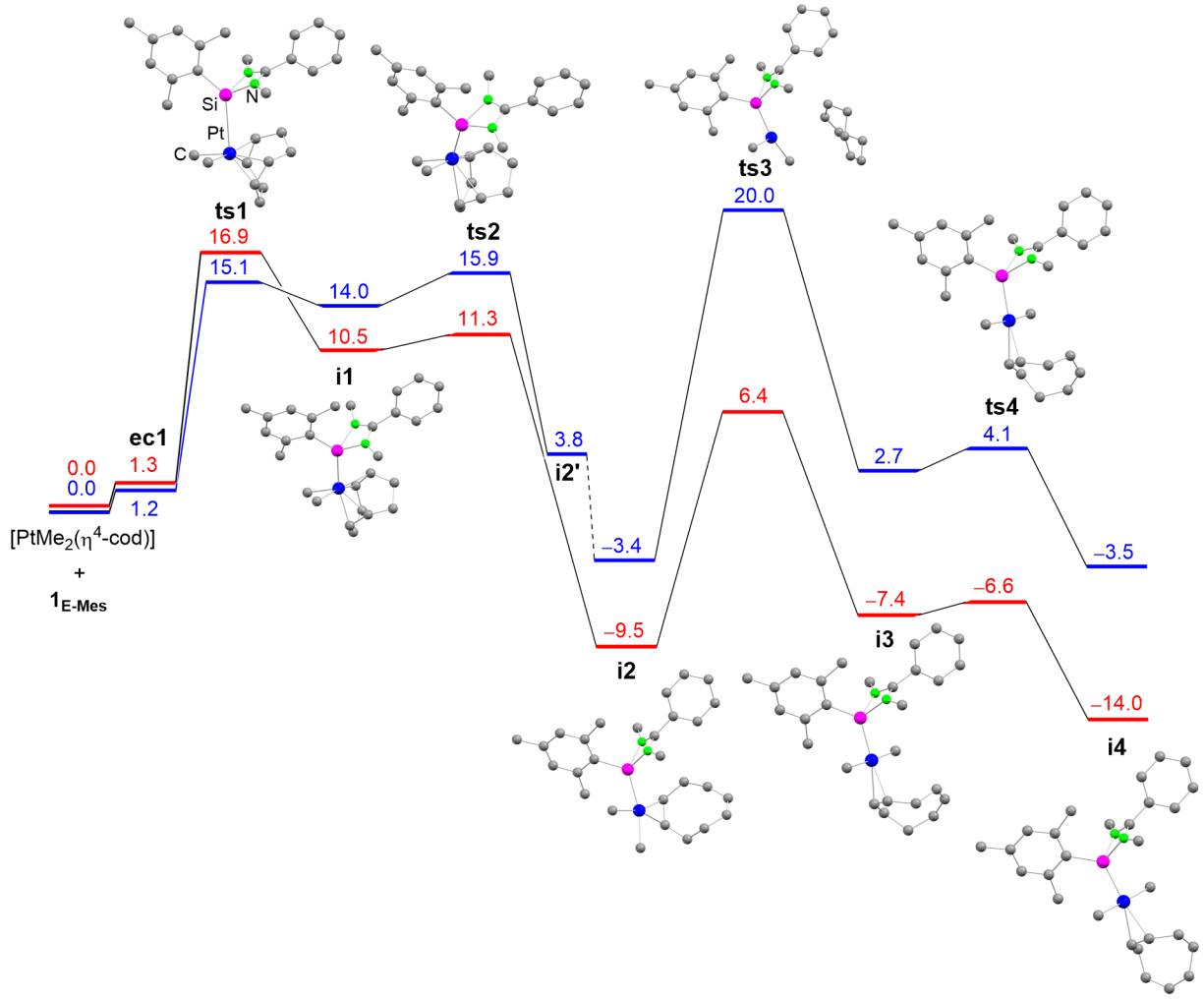

Figure 5. Relative energy profiles (ΔG, kcal mol^{-1}; wb97xd/cc-pVDZ/SDD(Pt)/benzene level; red trace for E = Si; blue trace for E = Ge) and optimized structures (only those with E = Si are shown) of the stationary points involved in the

formation of *trans*-[$PtMe_2(\eta^4$-cod)(**1**$_{E\text{-}Mes}$)] (**i4**) from [$PtMe_2(\eta^4$-cod)] and **1**$_{E\text{-}Mes}$, via the intermediacy of *cis*-[$PtMe_2(\eta^4$-cod)(**1**$_{E\text{-}Mes}$)] (**i2**). The given energies are relative to those of the starting materials ([$PtMe_2(\eta^4$-cod)] + **1**$_{E\text{-}Mes}$).

Having *trans*-**2**$_{Si\text{-}Mes}$ and *cis*-**2**$_{Ge\text{-}Mes}$ in hand, the plausible[10] cyclometallation of their HT ligands was attempted (upon C–H bond activation of a mesityl methyl group). Initially, solutions of both complexes were heated (monitoring the reaction course by ^{1}H NMR); however, only mixtures of unidentified species were observed all the way upon heating at 50 ºC (*trans*-**2**$_{Si\text{-}Mes}$) or 70 ºC (*cis*-**2**$_{Ge\text{-}Mes}$) for 48 h. Following a different approach, both complexes were treated at room temperature with one equivalent of [$H(OEt_2)_2$][BARF]. These reactions led to the isostructural derivatives [Pt{E(^{t}Bu$_2$bzam)$C_6H_2(CH_2)Me_2$}{E(^{t}Bu$_2$bzam)Mes}][BARF] [E = Si (**3**$_{Si\text{-}Mes}$), Ge (**3**$_{Ge\text{-}Mes}$)] upon formal release of two equivalents of CH_4, whose cations are cyclometalated 14-electron complexes (Scheme 3). Unfortunately, some [^{t}Bu$_2$bzamH_2][BARF] (**4**), which could not be efficiently separated from **3**$_{Si\text{-}Mes}$ and **3**$_{Ge\text{-}Mes}$ (see Figures S5 and S6), was also formed during the reactions.[20] The relevant ^{1}H NMR signals of both **3**$_{Si\text{-}Mes}$ and **3**$_{Ge\text{-}Mes}$, which are comparable, were satisfactorily identified. The spectra clearly indicated the presence of two inequivalent HT ligands, one of them being cyclometalated, as evidenced by a platinated methylene signal (δ(^{1}H) 4.23 ppm (s, sat, J_{Pt-H} = 60 Hz, 2 H; **3**$_{Si\text{-}Mes}$), 4.37 ppm (s, sat, J_{Pt-H} = 57 Hz, 2 H; **3**$_{Ge\text{-}Mes}$).

Scheme 3. Protonation Reactions of 2$_{Si\text{-}X}$ and 2$_{Ge\text{-}X}$

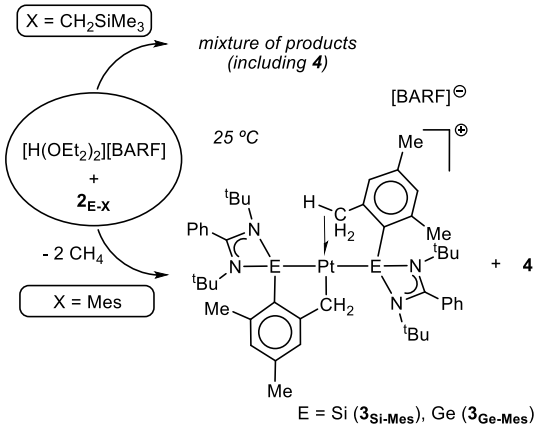

Taking into consideration the above results, the same acid was reacted with the CH_2SiMe_3 analogues *trans*-**2**$_{Si\text{-}Tmsm}$ and *cis*-**2**$_{Ge\text{-}Tmsm}$ (the C–H bond activation of a CH_2SiMe_3 methyl group would also render a 5-membered platinacycle). Unfortunately, only mixtures containing **4** and other unidentified species (no platinacycles) were observed in the crude reaction mixtures by ^{1}H NMR.

Compound **4**, [^{t}Bu$_2$bzamH$_2$][BARF], inevitably formed in the reactions of *trans*-$\mathbf{2}_{\mathbf{Si\text{-}R}}$ and *cis*-$\mathbf{2}_{\mathbf{Ge\text{-}R}}$ (R = Mes, Tmsm) with [H(OEt$_2$)$_2$][BARF], was isolated from the reaction mixtures and further characterized, also by X-ray crystallography (see Figure S8).[20]

Definitive proof of the structural identity of $\mathbf{3}_{\mathbf{Si\text{-}Mes}}$ and $\mathbf{3}_{\mathbf{Ge\text{-}Mes}}$ was obtained from an X-ray diffraction analysis of $\mathbf{3}_{\mathbf{Ge\text{-}Mes}}$. Its cationic part (Figure 6) is a square-planar platinum(II) complex featuring two germylenes in a *trans* disposition and two platinagermacyclopentene rings. The cation is crystallographically centrosymmetric because both germylene ligands are disordered into two positions with equal occupancy. One platinagermacyclopentene ring arises from the cyclometallation of one germylene ligand (Ge1) and the other results from agostic Pt···CH$_3$ interactions involving one mesityl methyl group of the other germylene (Ge1*). Similar structural features, including the Pt–CH$_2$ and Pt···CH$_3$ distances, have been reported for the cationic platinum(II) bis(phosphane) complexes [Pt{PR$_2$(C$_6$H$_2$(CH$_2$)Me$_2$)}{PR$_2$(Mes)}]$^+$ (R = isopropyl,[24] cyclohexyl[25]).

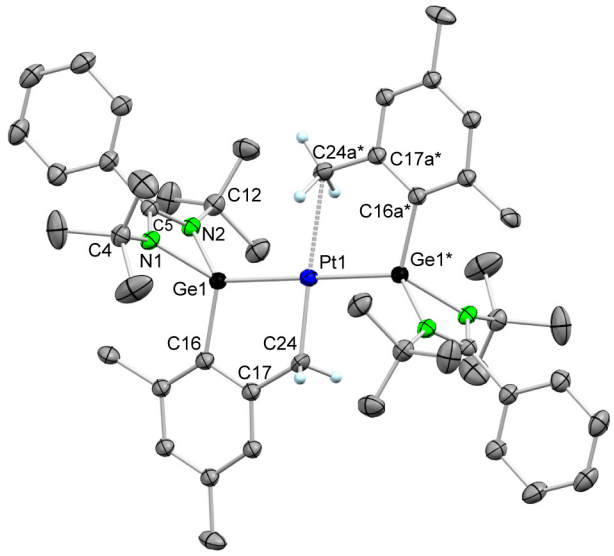

Figure 6. Structure of the cation of compound $\mathbf{3}_{\mathbf{Ge\text{-}Mes}}$ (25% displacement ellipsoids, H atoms have been omitted for clarity except for those on carbon atoms labelled as C24 and C24a*). The structure is centrosymmetric. The mesityl groups are disordered in two positions with equal occupancy. Only one of these two positions is shown in order to display a cyclometalated and a non-cyclometalated mesityl groups. Selected bond lengths (Å) and angles (°): Pt1−C24 2.02(1), Pt1···C24a* 2.54(2), Pt1−Ge1 2.3723(5), Ge1−C16 1.94(3), Ge1*−C16a* 1.96(3), Ge1−N1 1.933(4), Ge1−N2 1.944(3), N1−C4 1.481(6), N1−C5 1.340(5), N2−C5 1.330(5), N2−C12 1.477(5), C5−C6 1.490(5), C16−C17 1.41(2), C17−C24 1.53(2), C16a*−C17a* 1.40(2), C17a*−C24a* 1.53(2), Ge1−Pt1−Ge1* 180.0, C24−Pt1−Ge1 81.0(5), C24a*−Pt1−Ge1* 77.7(4), Pt1−Ge1−N1 124.7(1), Pt1−Ge1−N2 126.4(1), C16−Ge1−Pt1 105.1(8), C16a*−Ge1−Pt1 109.2(8), C16−Ge1−N1 116.1(7), C16a*−Ge1−N1 112.0(7), C16−Ge1−N2 113.9(9), C16a*−Ge1−N2 111.4(9), N1−Ge1−N2 67.5(1), N1−C5−N2 107.6(3).

CONCLUDING REMARKS

This work, highlighting the great versatility of heavier tetrylenes, demonstrates that a simple modification of the E and/or X variables of isostructural benzamidinatotetrylenes (HTs), E(^{t}Bu$_2$bzam)X (**1$_{E\text{-}X}$**), leads to substantial changes in both reactivity and stereoselectivity.

Firstly, regardless of the steric bulk of the HT ligand (X = Mes or CH_2SiMe_3), the stereoselectivity of the reactions of [$PtMe_2(\eta^4$-cod)] with **1$_{E\text{-}X}$** seems to be dictated by the nature of the tetrel atom, since *trans* disubstituted products were obtained for the silylenes (**2$_{Si\text{-}X}$**) but *cis* for the germylenes (**2$_{Ge\text{-}X}$**). DFT calculations indicated that the different stereochemistry observed has possibly a kinetic origin, as the calculated relative stability of the *trans* and *cis* stereoisomers of **2$_{E\text{-}X}$** cannot explain the experimental results. Interestingly, DFT calculations have shown that, in these reactions, the *cis* to *trans* isomerization of the monosubsituted *cis*-[$PtMe_2(\eta^2$-cod)(**1$_{E\text{-}Mes}$**)] intermediates are easier for E = Si than for E = Ge, and this kinetic effect seems to dictate the fate of the reactions. The *trans* reaction stereoselectivity reported in this work for the reactions involving the silylene ligands is very rare, since it is known that the reactions of [$PtMe_2(\eta^4$-cod)] with two equivalents of phosphanes or NHCs of different steric bulk give exclusively *cis*-products upon cod displacement.

Secondly, while the above mentioned reactions, which are the first ones to combine HTs with [$PtMe_2(\eta^4$-cod)], did not render cyclometalated complexes, agostically-stabilized cyclometalated 14-electron platinum(II) cationic complexes have been isolated from reactions of the mesityl complexes **2$_{E\text{-}Mes}$** with [$H(OEt_2)_2$][BARF]. However, no platinacycles were formed in analogous reactions with the CH_2SiMe_3-equipped complexes **2$_{E\text{-}Tmsm}$**.

EXPERIMENTAL SECTION

General Procedures. Solvents were dried over sodium diphenyl ketyl and were distilled under argon before use. All reactions were carried out under argon in an MBraun glovebox and/or using Schlenk-vacuum line techniques. All reaction products were vacuum-dried for several hours prior to being weighed and analyzed. The metal complex [$PtMe_2(\eta^4$-cod)],[26] the amidinato-HTs $\mathbf{1}_{\mathbf{Si\text{-}Mes}}$,[10b] $\mathbf{1}_{\mathbf{Ge\text{-}Mes}}$,[13a] $\mathbf{1}_{\mathbf{Si\text{-}Tmsm}}$ [13b] and $\mathbf{1}_{\mathbf{Ge\text{-}Tmsm}}$,[13d] and $[H(OEt_2)_2][BAr_F]$[27] were prepared following published procedures. All remaining reagents were purchased from commercial suppliers. NMR spectra were run on Bruker NAV-400 and AV-300 instruments; the standards used were the residual protic solvent resonance for ^{1}H [$\delta(C_6HD_5) = 7.16$ ppm, $\delta(CHDCl_2) = 5.32$ ppm] and the solvent resonance for ^{13}C [$\delta(C_6D_6) = 128.06$ ppm, $\delta(CD_2Cl_2) = 53.84$ ppm]. Microanalyses were obtained with a FlashEA112 (Thermo-Finnigan) microanalyzer. High-resolution mass spectra (HRMS) were obtained with a Bruker Impact II mass spectrometer operating in the ESI-Q-ToF positive mode. Some of the found and required masses for the correct isotope pattern were more than 5 ppm apart (these results are provided to illustrate the best values obtained to date).

***trans*-[$PtMe_2${Si(^{t}Bu$_2$bzam)Mes}$_2$] (*trans*-$\mathbf{2}_{\mathbf{Si\text{-}Mes}}$).** Toluene (1 mL) was added to a mixture of $\mathbf{1}_{\mathbf{Si\text{-}Mes}}$ (76 mg, 0.2 mmol) and $[PtMe_2(\eta^4$-cod)] (0.1 mmol, 33 mg). The resulting orange solution was stirred at room temperature for 1 h. The solvent was removed under reduced pressure and the residue was washed with hexane (2 x 0.5 mL) to give a white solid. The solid was dissolved in toluene (0.4 mL) and the resulting solution was kept in the freezer (–20 °C) for 2 days. A crop of colourless crystals formed in solution, which was separated and washed with hexane (0.2 mL) to give ***trans*-$\mathbf{2}_{\mathbf{Si\text{-}Mes}}$** as a white crystalline solid after vacuum drying (78 mg, 79 %). Anal. (%) Calcd for $C_{50}H_{74}N_4PtSi_2$ (982.3985 amu): C, 61.13; H, 7.59; N, 5.70; found C, 61.04; H, 7.46; N, 5.55. (+)-ESI HRMS: found (calcd) *m*/*z* 951.4556 (951.4630) $[M - 2\ Me]^+$.^{1}H NMR (C_6D_6, 300.9 MHz, 298 K): δ 7.85–7.70 (m, 2 H, 2 C*H* of Ph and/or Mes), 7.35–7.28 (m, 2 H, 2 C*H* of Ph), 7.02–6.90 (m, 10 H, 10 C*H* of Ph and Mes), 3.76 (s, 3 H, CH_3 of Mes), 3.59 (s, 3 H, CH_3 of Mes), 2.90 (s, 6 H, 2 CH_3 of Mes), 2.22 (s, 6 H, 2 CH_3 of Mes), 1.36 (s, 36 H, 12 CH_3 of ^{t}Bu), 0.89 (m, sat, $J_{Pt–H} = 21$ Hz, 2 CH_3 of Pt–Me) ppm. ^{13}C{^{1}H} NMR (C_6D_6, 100.6 MHz, 298 K): δ 166.3 (N*C*N), 165.9 (N*C*N), 148.0, 143.5, 138.4, 133.8, 132.6, 132.0 (10 C_{ipso} of Ph and Mes), 129.8–125.7 (14 *C*H of Ph and Mes), 54.1 (4 *C* of ^{t}Bu), 31.0 (12 *C*H$_3$ of ^{t}Bu), 26.3 (1 *C*H$_3$ of Mes), 26.1 (1 *C*H$_3$ of Mes), 24.8 (2

*C*H$_3$ of Mes), 21.2 (2 *C*H$_3$ of Mes), –16.9 (s, sat, $J_{Pt–C}$ = 217 Hz, 2 *C*H$_3$ of Pt–Me) ppm. ^{29}Si{^{1}H} NMR (C$_6$D$_6$, 79.5 MHz, 298 K): δ 72.4 (s, 1 Si), 71.7 (s, 1 Si) ppm.

***trans*-[PtMe$_2${Si(*t*Bu$_2$bzam)CH$_2$SiMe$_3$}$_2$] (*trans*-2$_{Si-Tmsm}$).** Toluene (1 mL) was added to a mixture of **1**$_{Si-Tmsm}$ (69 mg, 0.2 mmol) and [PtMe$_2$(η^4-cod)] (0.1 mmol, 33 mg). The resulting orange solution was stirred at room temperature for 1 h. The solvent was removed under reduced pressure and the residue was dissolved in hexane/toluene (1:1) and the resulting solution was kept in the freezer (–20 °C) for 2 days. A crop of colourless crystals formed in solution, which was separated and washed with hexane (0.2 mL) to give ***trans*-2**$_{Si-Tmsm}$ as a white crystalline solid after vacuum drying (56 mg, 61 %). Anal. (%) Calcd for C$_{40}$H$_{74}$N$_4$PtSi$_4$ (918.4625 amu): C, 52.31; H, 8.12; N, 6.10; found C, 52.04; H, 7.96; N, 5.86. (+)-ESI HRMS: found (calcd) *m*/*z* 950.4556 (950.4979) [*M* + CH$_3$OH + H]$^+$. ^{1}H NMR (C$_6$D$_6$, 300.1 MHz, 298 K): δ 7.83–7.77(m, 2 H, 2 C*H* of Ph), 7.23–7.17 (m, 2 H, C*H* of Ph), 6.95–6.84 (m, 6 H, C*H* of Ph), 1.32 (s, 36 H, 12 C*H*$_3$ of *t*Bu), 1.01 (m, 6 H, 2 C*H*$_3$ of Pt–Me$_2$), 0.94 (s, 4H, 2 C*H*$_2$SiMe$_3$), 0.51 (s, 18 H, 2 Si*M*e$_3$) ppm. ^{13}C{^{1}H} NMR (C$_6$D$_6$, 100.6 MHz, 299 K): δ 166.3 (2 N*C*N), 133.4–127.8 (10 *C*H + 2 *C*$_{ipso}$ of Ph), 53.7 (4 *C* of *t*Bu), 31.3 (12 *C*H$_3$ of *t*Bu), 7.6 (2 *C*H$_2$ of CH$_2$SiMe$_3$), 2.7 (6 *C*H$_3$ of CH$_2$SiMe$_3$), –12.4 (s, sat, $J_{Pt–C}$ = 210 Hz, 2 *C*H$_3$ of Pt–*Me*) ppm.

***cis*-[PtMe$_2${Ge(*t*Bu$_2$bzam)Mes}$_2$] (*cis*-2$_{Ge-Mes}$).** Toluene (1 mL) was added to a mixture of **1**$_{Ge-Mes}$ (85 mg, 0.2 mmol) and [PtMe$_2$(η^4-cod)] (0.1 mmol, 33 mg). The resulting yellow solution was stirred at room temperature for 1 h. The solvent was removed under reduced pressure and the residue was washed with hexane (2 x 0.5 mL) to give ***cis*-2**$_{Ge-Mes}$ as a white solid after vacuum drying (66 mg, 62 %). Anal. (%) Calcd for C$_{50}$H$_{74}$N$_4$Ge$_2$Pt (1071.4475 amu): C, 56.05; H, 6.96; N, 5.23; found C, 56.30; H, 6.55; N, 5.01 (although these results are outside the accepted range of analytical purity, they are provided to illustrate the best values obtained to date). (+)-ESI HRMS: found (calcd) *m*/*z* 1058.3700 (1058.3750) [*M* – Me]$^+$.^{1}H NMR (C$_6$D$_6$, 300.9 MHz, 298 K): δ 7.70–7.63 (m, 2 H, C*H* of Ph), 7.36–7.30 (m, 2 H, C*H* of Ph), 7.05–6.92 (m, 6 H, 6 C*H* of Ph), 6.94 (2, 4 H, 4 C*H* of Mes), 3.26 (s, br, 12 H, 4 C*H*$_3$ of Mes), 2.20 (s, 6 H, 2 C*H*$_3$ of Mes), 1.57 (s, sat, $J_{Pt–H}$= 27 Hz, 6 H, 2 C*H*$_3$ of Pt–Me), 1.13 (s, br, 36 H, 12 C*H*$_3$ of *t*Bu) ppm. ^{13}C{^{1}H} NMR (C$_6$D$_6$, 100.6 MHz, 299 K): δ 167.0 (2 N*C*N), 144.9, 137.9, 135.9 (10 *C*$_{ipso}$ of Ph and Mes), 130.1–127.6 (14 *C*H of Ph and Mes), 54.2 (4 *C* of *t*Bu), 32.0 (12 *C*H$_3$ of *t*Bu), 25.8 (s, br, 4 *C*H$_3$ of Mes), 21.2 (2 *C*H$_3$ of Mes), –1.91 (s, sat, $J_{Pt–C}$ = 305 Hz, 2 *C*H$_3$ of Pt–Me) ppm.

***cis*-[PtMe$_2${Ge(^{t}Bu$_2$bzam)CH$_2$SiMe$_3$}$_2$] (*cis*-2$_{Ge\text{-}Tmsm}$).** Toluene (1 mL) was added to a mixture of **1**$_{Ge\text{-}Tmsm}$ (78 mg, 0.2 mmol) and [PtMe$_2$(η^4-cod)] (0.1 mmol, 33 mg). The resulting yellow solution was stirred at room temperature for 1 h. The solvent was removed under reduced pressure and the residue was dissolved in hexane/toluene (1:1) and the resulting solution was kept in the freezer (–20 °C) for 2 days. A crop of colourless crystals formed in solution, which was separated and washed with hexane (0.2 mL) to give ***cis*-2**$_{Ge\text{-}Tmsm}$ as a white crystalline solid after vacuum drying (40 mg, 40 %). Anal. (%) Calcd for $C_{40}H_{74}N_4Ge_2PtSi_2$ (1007.5115 amu): C, 47.68; H, 7.40; N, 5.56; found C, 47.57; H, 7.18; N, 5.40. (+)-ESI HRMS: found (calcd) *m*/*z* 994.3299 (994.3289) [*M* – Me]$^+$. ^{1}H NMR (C_6D_6, 400.1 MHz, 298 K): δ 7.77–7.73 (m, 2 H, C*H* of Ph), 7.37–7.33 m, 2 H, C*H* of Ph), 7.02–6.97 (m, 6 H, C*H* of Ph), 1.51 (s, sat, $J_{Pt–H}$ = 36 Hz, 6 H, 2 CH_3 of Pt–Me), 1.24 (s, 36 H, 12 CH_3 of ^{t}Bu), 1.10 (s, 4H, CH_2SiMe$_3$), 0.50 (s, 18 H, Si*M*e$_3$) ppm. ^{13}C{^{1}H} NMR (C_6D_6, 100.6 MHz, 298 K): δ 167.6 (2 N*C*N), 135.4–127.3 (10 *C*H + 2 C_{ipso} of Ph), 53.9 (4 *C* of ^{t}Bu), 31.9 (12 *C*H$_3$ of ^{t}Bu), 21.4 (2 *C*H$_2$ of CH$_2$SiMe$_3$), 2.9 (6 *C*H$_3$ of CH$_2$SiMe$_3$), 1.41 (s, sat, $J_{Pt–C}$ = 328 Hz, 2 *C*H$_3$ of Pt–Me) ppm.

[Pt{Si(^{t}Bu$_2$bzam)C$_6$H$_2$(CH$_2$)Me$_2$}{Si(^{t}Bu$_2$bzam)Mes}][BARF] (3$_{Si\text{-}Mes}$). A J. Young NMR tube was loaded with *trans*-**2**$_{Si\text{-}Mes}$ (39 mg, 0.04 mmol), [H(OEt$_2$)$_2$][BAr$_F$] (41 mg, 0.04 mmol) and C_6D_6 (0.3 mL). The resulting yellow solution was stirred at room temperature for 30 min. The solvent was removed under reduced pressure, the residue was dissolved in toluene/CH_2Cl_2 (0.2 mL/0.3 mL) and the resulting solution was kept in the freezer (–20 °C) for 5 days. A crop of colourless crystals was separated from the solution. They were washed with toluene (0.2 mL) to give a *ca*. 1:1 mixture of **3**$_{Si\text{-}Mes}$ and **4** (10 mg) after vacuum drying (^{1}H NMR analysis). (+)-ESI HRMS: *m*/*z* found 950.4427; calcd for $C_{48}H_{67}N_4PtSi_2$ [*M* – BARF]$^+$: 950.4552. ^{1}H NMR (**3**$_{Si\text{-}Mes}$; CD_2Cl_2, 400.1 MHz, 298 K): δ 7.76–7.44 (m, 22 H, C*H* of BARF), 7.21 (s, 1 H, C*H* of Mes), 7.13 (s, 1 H, C*H* of Mes), 6.97 (s, 1 H, C*H* of Mes), 6.88 (s, 1 H, C*H* of Mes), 4.23 (s, sat, $J_{Pt–H}$ = 60 Hz, 2 H, CH_2 of Pt–CH$_2$), 2.67 (s, 3 H, CH_3 of Mes), 2.56 (s, 6 H, 2 CH_3 of Mes), 2.37 (s, 3 H, CH_3 of Mes), 2.36 (s, 3 H, CH_3 of Mes), 1.20 (s, 18 H, 6 CH_3 of ^{t}Bu), 1.19 (s, 18 H, 6 CH_3 of ^{t}Bu) ppm. ^{19}F{^{1}H} NMR (CD_2Cl_2, 282.3 MHz, 299 K): δ –62.8 (s) ppm.

[Pt{Ge(^{t}Bu$_2$bzam)C$_6$H$_2$(CH$_2$)Me$_2$}{Ge(^{t}Bu$_2$bzam)Mes}][BARF] (3$_{Ge\text{-}Mes}$). A J. Young NMR tube was loaded with *cis*-**2**$_{Ge\text{-}Mes}$ (86 mg, 0.08 mmol), [H(OEt$_2$)$_2$][BAr$_F$] (71 mg, 0.07 mmol) and C_6D_6 (0.5 mL). The resulting yellow solution was stirred at room temperature for 30 min to give a

yellow suspension. The solid was separated by decantation and was washed with 1:1 hexane-toluene (0.5 mL) to give a *ca*. 1:0.1 mixture of $\mathbf{3}_{\mathbf{Ge\text{-}Mes}}$ and **4** (37 mg) after vacuum drying (^{1}H NMR analysis). (+)-ESI HRMS: *m*/*z* found 1042.3352; calcd for $C_{48}H_{67}N_4Ge_2Pt$ [*M* – BARF]$^+$: 1042.3437. ^{1}H NMR ($\mathbf{3}_{\mathbf{Ge\text{-}Mes}}$; CD_2Cl_2, 400.1 MHz, 298 K): δ 7.78-7.47 (m, 22 H, C*H* of Ph and BARF), 7.21 (s, 1 H, C*H* of Mes), 7.17 (s, 1 H, C*H* of Mes), 7.03 (s, 1 H, C*H* of Mes), 6.95 (s, 1 H, C*H* of Mes), 4.37 (s, sat, $J_{Pt–H}$ = 57 Hz, 2 H, CH_2 of Pt–CH_2), 2.76 (s, 3 H, CH_3 of Mes), 2.71 (s, 3 H, CH_3 of Mes), 2.65 (s, 3 H, CH_3 of Mes), 2.38 (s, 3 H, CH_3 of Mes), 2.35 (s, 3 H, CH_3 of Mes), 1.16 (s, 18 H, 6 CH_3 of ^{t}Bu), 1.12 (s, 18 H, 6 CH_3 of ^{t}Bu) ppm. ^{19}F{^{1}H} NMR (CD_2Cl_2, 282.3 MHz, 299 K): δ –62.8 (s) ppm.

[^{t}Bu$_2$bzamH$_2$][BARF] (4). A J. Young NMR tube was loaded with *cis*-$\mathbf{2}_{\mathbf{Ge\text{-}Tmsm}}$ (41 mg, 0.04 mmol), [H(OEt$_2$)$_2$][BARF] (41 mg, 0.04 mmol) and C_6D_6 (0.3 mL). The resulting orange solution was stirred at room temperature for 30 min. The solvent was removed under reduced pressure and the remaining residue was dissolved in hexane/CH_2Cl_2 (0.2 mL/0.3 mL). The resulting solution was kept in the freezer at –20 °C for 3 days. A crop of crystals was formed. They were separated by decantation and washed with hexane (0.3 mL) to give **4** as a colourless crystalline solid (10 mg, 23 %). ^{1}H NMR (CD_2Cl_2, 300.1 MHz, 298 K): δ 7.76–7.40 (m, 17 H, C*H* of Ph and BARF), 6.38 (s, 1 H, N*H*), 6.10 (s, 1 H, N*H*), 1.57 (s, 9 H, 3 CH_3 of ^{t}Bu), 1.27 (s, 9 H, 3 CH_3 of ^{t}Bu) ppm. ^{13}C{^{1}H} NMR (CD_2Cl_2, 100.6 MHz, 299 K): δ 165.7 (N*C*N), 162.2 (q, $J_{B–C}$ = 50 Hz, 4 B-C_{ipso} of BARF), 135.2 (8 *o*-*C*H of BARF), 134.2 (*C*H of Ph), 130.1 (2 *C*H of Ph), 129.3 (q, $J_{F–C}$ = 31 Hz, 8 *m*-C_{ipso} of BARF), 128.3 (2 *C*H of Ph), 125.0 (q, $J_{F–C}$ = 276 Hz, 8 *C*F$_3$ of BARF), 117.9 (4 *p*-*C*H of BARF), 59.9 (*C* of ^{t}Bu), 56.2 (*C* of ^{t}Bu), 31.2 (3 *C*H$_3$ of ^{t}Bu), 29.0 (3 *C*H$_3$ of ^{t}Bu) ppm. ^{19}F{^{1}H} NMR (CD_2Cl_2, 282.3 MHz, 299 K): δ –62.8 (s) ppm. The C_{ipso} signal of the amidinato Ph group was not observed, possibly due to overlapping with other signals.

X-ray Diffraction Analyses. Crystals of *trans*-$\mathbf{2}_{\mathbf{Si\text{-}Mes}}$·2($C_7H_8$), *trans*-$\mathbf{2}_{\mathbf{Si\text{-}Tmsm}}$, *cis*-$\mathbf{2}_{\mathbf{Ge\text{-}Mes}}$, *cis*-$\mathbf{2}_{\mathbf{Ge\text{-}Tmsm}}$, $\mathbf{3}_{\mathbf{Ge\text{-}Mes}}$ and **4** were analyzed by X-ray diffraction. A selection of crystal, measurement and refinement data is given in Table S1. Diffraction data were collected on an Oxford Diffraction Xcalibur Onyx Nova single crystal diffractometer with CuKα radiation. Empirical absorption corrections were applied using the SCALE3 ABSPACK algorithm as implemented in CrysAlisPro RED.[28] The structures were solved with SIR-97.[29] Isotropic and full matrix anisotropic least square refinements were carried out using SHELXL.[30] All non-H atoms were refined anisotropically. H atoms were set in calculated positions and were refined riding on their parent atoms except for those

on the N atoms of **4**, which were located in the corresponding Fourier map and were refined freely. One of the toluene molecules found in the asymmetric unit of *trans*-$\mathbf{2}_{\mathbf{Si\text{-}Mes}}$·2($C_7H_8$) was disordered over two positions with 53:47 occupancy ratio, requiring restraints on its geometrical and thermal parameters. The platinum bound methyl groups (C49 and C50) and the methyl groups of one of the *tert*-butyl moieties (quaternary carbon labelled as C28) of *cis*-$\mathbf{2}_{\mathbf{Ge\text{-}Mes}}$ were disordered over two positions with 51:49 and 58:42, respectively, occupancy ratios, requiring restraints on its geometrical and thermal parameters. The asymmetric unit of $\mathbf{3}_{\mathbf{Ge\text{-}Mes}}$ shows only half cation and half anion, as the Pt atom is located on a center of inversion and a C_2 axis passes through the B atom of the BARF moiety. The mesityl fragment found in the asymmetric unit of $\mathbf{3}_{\mathbf{Ge\text{-}Mes}}$ is disordered over two positions (50:50 occupancy ratio), requiring restraints on their thermal parameters (one position gives a cyclometalated mesityl through C24 and the other a noncyclometalated mesityl through C24a*). The fluorine atoms of the CF_3 groups of $\mathbf{3}_{\mathbf{Ge\text{-}Mes}}$ were disordered over two positions with 53:47 (on C31), 74:26 (on C32), 56:40 (on C40) and 51:49 (on C40) occupancy ratios, requiring restraints on their thermal parameters. The fluorine atoms of the CF_3 moieties of **4** were disordered over two positions with 59:41 (on C22), 71:29 (on C23), 60:40 (on C30), 53:47 (on C31), 51:49 (on C38), 61:39 (on C39), 66:34 (on C46) and 53:47 (on C47) occupancy ratios, requiring restraints on their geometrical parameters. The WINGX program system[31] was used throughout the structure determinations. The molecular plots were made with MERCURY.[32] The molecular plots were made with MERCURY.[32] CCDC deposition numbers: 1991462 (*trans*-$\mathbf{2}_{\mathbf{Si\text{-}Mes}}$ 2(C_7H_8)), 1991463 (*trans*-$\mathbf{2}_{\mathbf{Si\text{-}Tmsm}}$), 1991464 (*cis*-$\mathbf{2}_{\mathbf{Ge\text{-}Mes}}$), 1991465 (*cis*-$\mathbf{2}_{\mathbf{Ge\text{-}Tmsm}}$), 1991466 ($\mathbf{3}_{\mathbf{Ge\text{-}Mes}}$) and 1991467 (**4**).

Theoretical Calculations. DFT calculations were carried out using the wB97XD functional,[33] which includes the second generation of Grimme's dispersion interaction correction[34] as well as long-range interactions effects. The Stuttgart-Dresden relativistic effective core potentials and the associated basis sets (SDD) was used for the Pt[35] atoms. The basis set used for the remaining atoms was the cc-pVDZ.[36] All stationary points were fully optimized in gas phase and confirmed as energy minima (all positive eigenvalues) or transition states (one negative eigenvalue) by analytical calculation of frequencies. The electronic energies of the optimized structures were used to calculate the zero-point corrected energies and the enthalpic and entropic contributions via vibrational frequency calculations. Solvation free energies were obtained with the self-consistent reaction field (SCRF) for the standard continuum solvation model (CPCM),[37] by using the single-point solvation energy of the optimized structures and the thermodynamic correction from the gas phase

calculations. All Gibbs energies were computed at 298.15 K and 1.0 atm. All calculations were carried out with the Gaussian09 package.[38]

ASSOCIATED CONTENT

The Supporting Information is available free of charge on the ACS Publications website at DOI: 10.1021/acs.organomet.xxxxxxx.

Crystal, acquisition, and refinement XRD data, ^{1}H and $^{13}C\{^{1}H\}$ NMR spectra of *trans*-$\mathbf{2}_{\mathbf{Si\text{-}Mes}}$, *trans*-$\mathbf{2}_{\mathbf{Si\text{-}Tmsm}}$, *cis*-$\mathbf{2}_{\mathbf{Ge\text{-}Mes}}$, *cis*-$\mathbf{2}_{\mathbf{Ge\text{-}Tmsm}}$, $\mathbf{3}_{\mathbf{Si\text{-}Mes}}$, $\mathbf{3}_{\mathbf{Ge\text{-}Mes}}$ and **4**; images and metric parameters of the DFT-optimized molecules *trans*-$\mathbf{2}_{\mathbf{Si\text{-}Mes}}$, *trans*-$\mathbf{2}_{\mathbf{Si\text{-}Tmsm}}$, *cis*-$\mathbf{2}_{\mathbf{Ge\text{-}Mes}}$, *cis*-$\mathbf{2}_{\mathbf{Ge\text{-}Tmsm}}$, *cis*-$\mathbf{2}_{\mathbf{Si\text{-}Mes}}$, *cis*-$\mathbf{2}_{\mathbf{Si\text{-}Tmsm}}$, *trans*-$\mathbf{2}_{\mathbf{Ge\text{-}Mes}}$ and *trans*-$\mathbf{2}_{\mathbf{Ge\text{-}Tmsm}}$ (PDF).

X-ray crystallographic data (CIF).

Atomic coordinates for all the DFT-optimized structures (XYZ).

AUTHOR INFORMATION

Corresponding Author

*E-mail for J.A.C.: jac@uniovi.es

*E-mail for P.G.-A.: pga@uniovi.es

Notes

The authors declare no competing financial interest.

ACKNOWLEDGMENTS

This work was supported by MINECO-FEDER projects CTQ2016-75218-P and CTQ2016-81797-REDC.

REFERENCES

(1) For reviews on the general transition-metal chemistry of HTs, see: (a) Tacke, R.; Ribbeck, T. Bis(amidinato)- and bis(guanidinato)silylenes and silylenes with one sterically demanding amidinato or guanidinato ligand: synthesis and reactivity. *Dalton Trans*. **2017**, *46*, 13628–13659. (b) Corey, J. Y. Reactions of Hydrosilanes with Transition Metal Complexes. *Chem. Rev*. **2016**, *116*, 11291–11435. (c) Cabeza, J. A.; García-Álvarez, P.; Polo, D. Intramolecularly Stabilized Heavier Tetrylenes: From Monodentate to Bidentate Ligands. *Eur. J. Inorg. Chem*. **2016**, *2016*,

10–22. (d) Álvarez-Rodríguez, L.; Cabeza, J. A.; García-Álvarez, P.; Polo, D. Álvarez-Rodríguez, L.; Cabeza, J. A.; García-Álvarez, P.; Polo, D. The transition-metal chemistry of amidinatosilylenes, -germylenes and -stannylenes. *Coord. Chem. Rev.* **2015**, *300*, 1–28. (e) Baumgartner, J.; Marschner, C. Coordination of non-stabilized germylenes, stannylenes, and plumbylenes to transition metals. *Rev. Inorg. Chem.* **2014**, *34*, 119–152. (f) Blom, B.; Stoelzel, M.; Driess, M. New Vistas in N-Heterocyclic Silylene (NHSi) Transition-Metal Coordination Chemistry: Syntheses, Structures and Reactivity towards Activation of Small Molecules. *Chem. Eur. J.* **2013**, *19*, 40–62. (g) Waterman, R.; Hayes, P. G.; Tilley, T. D. Development and Chemical Reactivity of Transition-Metal Silylene Complexes. *Acc. Chem. Res.* **2007**, *40*, 712–719. (h) Okazaki, M.; Tobita, H.; Ogino, H. Reactivity of silylene complexes. *Dalton Trans.* **2003**, 493–506. (i) Lappert, M. F.; Rowe, R. S. The role of group 14 element carbene analogues in transition metal chemistry. *Coord. Chem. Rev.* **1990**, *100*, 267–292. (j) Petz, W. Transition-metal complexes with derivatives of divalent silicon, germanium, tin, and lead as ligands. *Chem. Rev.* **1986**, *86*, 1019–1047. (k) Lappert, M. F.; Power, P. P. Subvalent group 4B metal alkyls and amides. Part 7. Transition-metal chemistry of metal(II) bis(trimethylsilyl)amides M′$(NR_2)_2$(R = $SiMe_3$; M′= Ge, Sn, or Pb). *J. Chem. Soc. Dalton Trans.* **1985**, 51–57.

(2) For reviews on HT transition-metal complexes in catalysis, see: (a) Zhou, Y.-P.; Driess, M. Isolable Silylene Ligands Can Boost Efficiencies and Selectivities in Metal-Mediated Catalysis. *Angew. Chem., Int. Ed.* **2019**, *58*, 3715–3728. (b) Raoufmoghaddam, S.; Zhou, Y.-P.; Wang, Y.; Driess, M. N-heterocyclic silylenes as powerful steering ligands in catalysis. *J. Organomet. Chem.* **2017**, *829*, 2–10. (c) Blom, B.; Gallego, D.; Driess, M. N-heterocyclic silylene complexes in catalysis: new frontiers in an emerging field. *Inorg. Chem. Front.* **2014**, *1*, 134–148.

(3) See, for example: (a) Benedek, Z.; Szilvási, T. Theoretical Assessment of Low-Valent Germanium Compounds as Transition Metal Ligands: Can They Be Better than Phosphines or NHCs? *Organometallics* **2017**, *36*, 1591–1600. (b) Benedek, Z.; Szilvási, T. Can low-valent silicon compounds be better transition metal ligands than phosphines and NHCs? *RSC Adv.* **2015**, *5*, 5077–5086.

(4) For reviews on the fundamental aspects of cyclometallation, see: (a) Omae, I. *Cyclometalation Reactions: Five- Membered Ring Products as Universal Reagents*, Springer: New York, 2014. (b) Albrecht, M. Cyclometalation Using d-Block Transition Metals: Fundamental Aspects and Recent

Trends. *Chem. Rev.* **2010**, 110, 576–623. (c) Omae, I. Intramolecular five-membered ring compounds and their applications. *Coord. Chem. Rev.* **2004**, *248*, 995–1023. (d) Canty, A. J.; van Koten, G. Mechanisms of d^8 organometallic reactions involving electrophiles and intramolecular assistance by nucleophiles. *Acc. Chem. Res.* **1995**, *28*, 406–413. (e) Ryabov, A. D. Mechanisms of intramolecular activation of carbon-hydrogen bonds in transition-metal complexes. *Chem. Rev.* **1990**, *90*, 403–424.

(5) For selected reviews, see: (a) Wanga, C.; Xiao, J. Iridacycles for hydrogenation and dehydrogenation reactions. *Chem. Commun.* **2017**, *53*, 3399–3411. (b) Kumar, R.; Nevado, C. Cyclometalated Gold(III) Complexes: Synthesis, Reactivity, and Physicochemical Properties. *Angew. Chem. Int. Ed.* **2017**, *56*, 1994–2015. (c) Bruneau, A.; Roche, M.; Alami, M.; Messaoudi, S. 2-Aminobiphenyl Palladacycles: The "Most Powerful" Precatalysts in C–C and C–Heteroatom Cross-Couplings. *ACS Catal.* **2015**, *5*, 1386–1396. (d) Alonso, D. A.; Nájera, C. Oxime-derived palladacycles as source of palladium nanoparticles. *Chem. Soc. Rev.* **2010**, *39*, 2891–2902. (e) Djukic, J.-P.; Sortais, J.-B.; Barloy, L.; Pfeffer, M. Cycloruthenated Compounds – Synthesis and Applications. *Eur. J. Inorg. Chem.* **2009**, *2009*, 817–853. (f) *Palladacycles, Synthesis, Characterization and Applications*; Dupont, J.; Pfeffer, M., Eds.; Wiley-VCH: Weinheim, Germany, 2008. (g) Beletskaya, I. P.; Cheprakov, A. V. Palladacycles in catalysis – a critical survey.*J. Organomet. Chem.* **2004**, *689*, 4055–4082. (h) van der Boom, M. E.; Milstein, D. Cyclometalated Phosphine-Based Pincer Complexes: Mechanistic Insight in Catalysis, Coordination, and Bond Activation. *Chem. Rev.* **2003**, *103*, 1759–1792. (i) Bedford, R. B. Palladacyclic catalysts in C–C and C–heteroatom bond-forming reactions. *Chem. Commun.* **2003**, 1787–1796. (j) Singleton, J. T. The uses of pincer complexes in organic synthesis. *Tetrahedron* **2003**, *59*, 1837–1857. (k) Albrecht, M.; van Koten, G. Platinum Group Organometallics Based on "Pincer" Complexes: Sensors, Switches, and Catalysts. *Angew. Chem. Int. Ed.* **2001**, *40*, 3750–3781.

(6) For recent reviews, see: (a) Caporale, C.; Massi, M. Cyclometalated iridium(III) complexes for life science. *Coord. Chem. Rev.* **2018**, *363*, 71–91. (b) Omae, I. Applications of five-membered ring products of cyclometalation reactions as anticancer agents. *Coord. Chem. Rev.* **2014**, *280*, 84–95.

(7) For selected reviews, see: (a) Omae, I. Application of five-membered ring products of cyclometalation reactions as sensing materials in sensing devices. *J. Organomet. Chem.* **2016**, *823*, 50–75. (b) Omae, I. Application of the five-membered ring blue light-emitting iridium products of cyclometalation reactions as OLEDs. *Coord. Chem. Rev.* **2016**, *310*, 154–169. (c) Strassner, T. Phosphorescent Platinum(II) Complexes with C∧C* Cyclometalated NHC Ligands. *Acc. Chem. Res.* **2016**, *49*, 2680–2689. (d) Fan, C.; Yang, C. Yellow/orange emissive heavy-metal complexes as phosphors in monochromatic and white organic light-emitting devices. *Chem. Soc. Rev.* **2014**, *43*, 6439–6469. (e) Bomben, P. G.; Robson, K. C. D.; Koivisto, B. D.; Berlinguette, C. P. Cyclometalated ruthenium chromophores for the dye-sensitized solar cell. *Coord. Chem. Rev.* **2012**, *256*, 1438–1450. (f) Williams, J. A. G. The coordination chemistry of dipyridylbenzene: N-deficient terpyridine or panacea for brightly luminescent metal complexes? *Chem. Soc. Rev.* **2009**, *38*, 1783–1801. (g) *Highly Efficient OLEDs with Phosphorescent Materials*; Yersin, H., Ed.; Wiley-VCH: Weinheim, 2008. (h) Bruce, D. W.; Deschenaux, R.; Donnio, B.; Guillon, D. *Comprehensive Organometallic Chemistry III*; Mingos, D. M. P.; Crabtree, R. H., Eds.; Elsevier: Amsterdam, The Netherlands, 2007, vol. 12, p. 217. (i) Albert, J.; Granell, J.; Muller, G. Synthesis and applications of optically active metallacycles derived from primary amines. *J. Organomet. Chem.* **2006**, *691*, 2101–2106.

(8) (a) Bakthavachalam, K.; Dutta, S.; Arivazhagan, C.; Raghavendra, B.; Haridas, A.; Sen, S. S.; Koley, D.; Ghosh, S. Cyclometallation of a germylene ligand by concerted metalation–deprotonation of a methyl group. *Dalton Trans.* **2018**, *47*, 15835–15844. (b) Hawkins, S. M.; Hitchcock, P. B.; Lappert, M. F.; Rai, A. K. Iridium(III) Hydrides derived from an Iridium(I) Substrate by Oxidative Addition and Cyclometallation of Germanium(II) Bis(trimethyisily1)amide; X-Ray Structures of [{$CH_2Me_2SiN(R)(NR_2)Ge$}$HIr(\mu$-$Cl)_2${$Ge(NR_2)N(R)SiMe_2CH_2$}IrH{$Ge(NR_2)_2$}] and [Ir{$GeCl(NR_2)N(R)SiMe_2CH_2$}$(CO)_2H${$Ge(NR_2)$}](R = $SiMe_3$). *J. Chem. Soc. Chem. Commun.* **1986**, 1689–1690.

(9) (a) Gallego, D.; Brück, A.; Irran, E.; Meier, F.; Kaupp, M.; Driess, M.; Hartwig, J. F. From Bis(silylene) and Bis(germylene) Pincer-Type Nickel(II) Complexes to Isolable Intermediates of the Nickel-Catalyzed Sonogashira Cross-Coupling Reaction. *J. Am. Chem. Soc.* **2013**, *135*, 15617–15626. (b) Brück, A.; Gallego, D.; Wang, W.; Irran, E.; Driess, M.; Hartwig, J. F. Pushing the σ-

Donor Strength in Iridium Pincer Complexes: Bis-(silylene) and Bis(germylene) Ligands Are Stronger Donors than Bis(phosphorus(III)) Ligands. *Angew. Chem. Int. Ed.* **2012**, *51*, 11478–11482. (c) Wang, W.; Inoue, S.; Irran, E.; Driess, M. Synthesis and Unexpected Coordination of a Silicon(II)-Based SiCSi Pincerlike Arene to Palladium. *Angew. Chem. Int. Ed.* **2012**, *51*, 3691–3694. (d) Li, S.; Wang, Y.; Yang, W.; Li, K.; Sun, H.; Li, X.; Fuhr, O.; Fenske, D. N_2 Silylation Catalyzed by a Bis(silylene)-Based [SiCSi] Pincer Hydrido Iron(II) Dinitrogen Complex. *Organometallics* **2020**, *39*, 757–766.

(10) (a) Cabeza, J. A.; Fernández-Colinas, J. M.; García-Álvarez, P.; González-Álvarez, L. Pérez-Carreño, E. Mesityl(amidinato)tetrylenes as ligands in iridium(I) and iridium(III) complexes: silicon versus germanium and simple κ^1-coordination versus cyclometallation. *Dalton Trans.* **2019**, *48*, 10996–11003. (b) Cabeza, J. A.; García-Álvarez, P.; González-Álvarez, L. Facile cyclometallation of a mesitylsilylene: synthesis and preliminary catalytic activity of iridium(III) and iridium(V) iridasilacyclopentenes. *Chem. Commun.* **2017**, *53*, 10275–10278.

(11) See, for example: (a) Schmid, G.; Balk, H. J. Silylenes as Ligands in Platin Complexes. *Chem. Ber.* **1970**, *103*, 2240–2244. (b) Marks, T. J. Dialkylgermylene- and -stannylene-Pentacarbonylchromium Complexes. *J. Am. Chem. Soc.* **1971**, *93*, 7090–7091.

(12) See, for example: (a) Cabeza, J. A.; Damonte, M.; García-Álvarez, P.; Pérez-Carreño, E. E. Easy abstraction of a hydride anion from an alkyl C–H bond of a coordinated bis(N-heterocyclic carbene). *Chem. Commun.* **2013**, *49*, 2813–2815. (b) Cabeza, J. A.; del Río, I.; Pérez-Carreño, E.; Sánchez-Vega, M. G.; Vázquez-García, D. A Simple Preparation of Pyridine-Derived N-Heterocyclic Carbenes and Their Transformation into Bridging Ligands by Orthometalation. *Angew. Chem. Int. Ed.* **2009**, *48*, 555–558. (c) Cabeza, J. A.; da Silva, I.; del Río, I.; Martínez-Méndez, L.; Miguel, D.; Riera, V. Activation of All Bonds of a Methyl Group Attached to an Organic Fragment. *Angew. Chem. Int. Ed.* **2004**, *43*, 3464–3467. (d) Rothwell, I. P. Cyclometalation Chemistry of Aryl Oxide Ligation. *Acc. Chem. Res.* **1988**, *21*, 153–159.

(13) See, for example: (a) Cabeza, J. A.; García-Álvarez, P.; Gómez-Gallego, M.; González-Álvarez, L.; Merinero, A. D.; Sierra, M. A. Two Types of σ-Allenyl Complexes from Reactions of Silylenes and Germylenes with Chromium Fischer Alkynyl(alkoxy)carbenes. *Chem. Eur. J.* **2019**, *25*, 8635–8642. (b) Cabeza, J. A.; García-Álvarez, P.; Gómez-Gallego, M.; González-Álvarez, L.;

Merinero, A. D.; Sierra, M. A. Unexpected Zwitterionic Allenyls from Silylenes and a Fischer Alkynylcarbene: A Remarkable Silylene-Promoted Rearrangement. *Chem. Eur. J.* **2019**, *25*, 2222–2225. (c) Álvarez-Rodríguez, L.; Cabeza, J. A.; García-Álvarez, P.; Gómez-Gallego, M.; González-Álvarez, L.; Merinero, A. D.; Sierra, M. A. Reversible Carbene Insertion into a Ge–N Bond and Insights into CO and Carbene Substitution Reactions Involving Amidinatogermylenes and Fischer Carbene Complexes. *Chem. Eur. J.* **2019**, *25*, 1588–1594. (d) Álvarez-Rodríguez, L.; Cabeza, J. A.; García-Álvarez, P.; Pérez-Carreño, E. Ruthenium Carbene Complexes Analogous to Grubbs-I Catalysts Featuring Germylenes as Ancillary Ligands. *Organometallics* **2018**, *37*, 3399–3406. (e) Álvarez-Rodríguez, L.; Cabeza, J. A.; García-Álvarez, P.; Gómez-Gallego, M.; Merinero, A. D.; Sierra, M. A. . First Insertions of Carbene Ligands into Ge–N and Si–N Bonds. *Chem. Eur. J.* **2017**, *23*, 4287–4291. (f) Álvarez-Rodríguez, L.; Cabeza, J. A.; Fernández-Colinas, J. M.; García-Álvarez, P.; Polo, D. Amidinatogermylene Metal Complexes as Homogeneous Catalysts in Alcoholic Media. *Organometallics* **2016**, *35*, 2516–2523. (g) Cabeza, J. A.; García-Álvarez, P.; Gobetto, R.; González-Álvarez, L.; Nervi. C.; Pérez-Carreño, E.; Polo, D. $[MnBrL(CO)_4]$ (L = Amidinatogermylene): Reductive Dimerization, Carbonyl Substitution, and Hydrolysis Reactions. *Organometallics* **2016**, *35*, 1761–1770. (h) Álvarez-Rodríguez, L.; Cabeza, J. A.; García-Álvarez, P.; Polo, D. Amidinatogermylene Complexes of Copper, Silver, and Gold. *Organometallics* **2015**, *34*, 5479–5484. (i) Cabeza, J. A.; Fernández-Colinas, J. M.; García-Álvarez, Pérez-Carreño, E.; Polo. D. Reactivity Studies on a Binuclear Ruthenium(0) Complex Equipped with a Bridging κ^2*N*,*Ge*-Amidinatogermylene Ligand. *Inorg. Chem.* **2015**, *54*, 4850–4861.

(14) See, for example: (a) Cabeza, J. A.; García-Álvarez, P.; Pérez-Carreño, E.; Polo, D. Ring Opening and Bidentate Coordination of Amidinate Germylenes and Silylenes on Carbonyl Dicobalt Complexes: The Importance of a Slight Difference in Ligand Volume. *Chem. Eur. J.* **2014**, *20*, 8654–8663. (b) Nguyen. T. A. N.; Frenking, G. Transition-Metal Complexes of Tetrylones $[(CO)_5W\text{-}E(PPh_3)_2]$ and Tetrylenes $[(CO)_5W\text{-}NHE]$ (E = C–Pb): A Theoretical Study. *Chem. Eur. J.* **2012**, *18*, 12733–12748. (c) Boehme, C.; Frenking, G. N-Heterocyclic Carbene, Silylene, and Germylene Complexes of MCl (M = Cu, Ag, Au). A Theoretical Study. *Organometallics*, **1998**, *17*, 5801–5809.

(15) For crystallographically characterized Pt complexes equipped with terminal silylenes, see: (a) Troadec, T.; Prades, A.; Rodriguez, R.; Mirgalet, R.; Baceiredo, A.; Saffon-Merceron, N.; Branchadell, V.; Kato, T. T. Silacyclopropylideneplatinum(0) Complex as a Robust and Efficient Hydrosilylation Catalyst. *Inorg. Chem.* **2016**, *55*, 8234–8240. (b) Iimura, T.; Akasaka, N.; Iwamoto, T. Dialkylsilylene-Pt(0) Complex with a DVTMS Ligand for the Catalytic Hydrosilylation of Functional Olefins. *Organometallics* **2016**, *35*, 4071–4076. (c) Baus, J. A.; Mück, F. M.; Bertermann, R.; Tacke, R. Homoleptic Two-Coordinate 14-Electron Palladium and Platinum Complexes with Two Bis(guanidinato)silylene Ligands. *Eur. J. Inorg. Chem.* **2016**, *2016*, 4867–4871. (d) Agou, T.; Sasamori, T.; Tokitoh, N. Synthesis of an Arylbromosilylene–Platinum Complex by Using a 1,2-Dibromodisilene As a Silylene Source. *Organometallics* **2012**, *31*, 1150–1154. (e) Watanabe, C.; Inagawa, Y.; Iwamoto, T.; Kira, M. Synthesis and structures of (dialkylsilylene)bis(phosphine)-nickel, palladium, and platinum complexes and (η^6-arene)(dialkylsilylene)nickel complexes. *Dalton Trans.* **2010**, *39*, 9414–9420. (f) Avent, A. G.; Gehrhus, B.; Hitchcock, P. B.; Lappert, M. F.; Maciejewski, H. Synthesis and characterisation of bis(amino)silylenes–nickel(0), –palladium(II), –platinum(0), –platinum(II) and copper(I) complexes. *J. Organomet. Chem.* **2003**, *686*, 321–331. (g) Gehrhus, B.; Hitchcock, P. B.; Lappert, M. F.; Maciejewski, H. Silylenenickel(0) or Silyl(silylene)platinum(II) Complexes by Reaction of Si[($NCH_2But)_2C_6H_4$-1,2] with [$NiCl_2(PPh_3)_2$], [$Ni(cod)_2$], or [$PtCl_2(PPh_3)_2$]. *Organometallics* **1998**, *17*, 5599–5601. (h) Feldman, J. D.; Mitchell, G. P.; Nolte, J.-O.; Tilley, T. D. Isolation and Characterization of Neutral Platinum Silylene Complexes of the Type $(R_3P)_2Pt{=}SiMes_2$ (Mes = 2,4,6-Trimethylphenyl). *J. Am. Chem. Soc.* **1998**, *120*, 11184–11185. (i) Grumbine, S. D.; Tilley, T. D.; Arnold, F. P.; Rheingold, A. L. A Fischer-type Silylene Complex of Platinum: [*trans*-$(Cy_3P)_2(H)Pt{=}Si(SEt)_2]BPh_4$. *J. Am. Chem. Soc.* **1993**, *115*, 7884–7885.

(16) For crystallographically characterized Pt complexes equipped with terminal germylenes, see: (a) Septelean, R.; Moraru, I.-T.; Kocsor, T.-G.; Deak, N.; Saffon-Merceron, N.; Castel, A.; Nemes, G. Computational and experimental investigation of phosphaalkenyl germylenes from donor-acceptor perspective. *Inorg. Chim. Acta* **2017**, *475*, 112–119. (b) Hupp, F.; Ma, M.; Kroll, F.; Oscar, F.; Jimenez-Halla, C.; Dewhurst, R. D.; Radacki, K.; Stasch, A.; Jones, C.; Braunschweig, H. Platinum Complexes Containing Pyramidalized Germanium and Tin Dihalide Ligands Bound through σ,σ M=E Multiple Bonds. *Chem. Eur. J.* **2014**, *20*, 16888–16898. (c) Sharma, M. K.; Singh,

D.; Mahawar, P.; Yadav, R.; Nagendran, S. Catalytic cyanosilylation using germylene stabilized platinum(II) dicyanide. *Dalton Trans*. **2018**, *47*, 5943–5947. (d) Litz, K. E.; Henderson, K.; Gourley, R.W.; Holl, M. M. B. Reversible Insertion Reactions of a Platinum Germylene Complex. *Organometallics* **1995**, *14*, 5008–5010.

(17) The platinum bound methyl groups (C49 and C50) of *cis*-$\mathbf{2}_{\mathbf{Ge\text{-}Mes}}$ were disordered over two positions with 51:49 occupancy ratio.

(18) (a) The range of Pt–C bond distances found for $[PtMe_2L_2]$ (L = any ligand) complexes, all of them with *cis* stereochemistry (172 examples), is 1.935–2.338 Å, with an average value of 2.087(2) Å (CSD version 5.40; updated May 2019); (*b*) See also, Allen F. H. The Cambridge Structural Database: a quarter of a million crystal structures and rising. *Acta Crystallogr. Sect. B*, 2002, **58**, 380.

(19) See, for example: Cabeza, J. A.; García-Álvarez, P.; Polo. D. Synthesis of Mixed Tin–Ruthenium and Tin–Germanium–Ruthenium Carbonyl Clusters from $[Ru_3(CO)_{12}]$ and Diaminometalenes (M = Sn, Ge). *Inorg. Chem*. **2012**, *51*, 2569–2576.

(20) See, for example: (a) Haar, C. M.; Nolan, S. P.; Marshall, W. J.; Moloy, K. G.; Prock, A.; Giering, W. P. Synthetic, Structural, and Solution Thermochemical Studies in the Dimethylbis(phosphine)platinum(II) System. Dichotomy between Structural and Thermodynamic Trends. *Organometallics* **1999**, *18*, 474–479.

(21) See, for example: (a) Ríos, P.; Fouilloux, H.; Vidossich, P.; Díez, J.; Lledós, A.; Conejero, S. Isolation of a Cationic Platinum(II) σ-Silane Complex. *Angew. Chem. Int. Ed*. **2018**, *57*, 3217 – 3221; (b) Fortman, G. C.; Slawin, A. M. Z.; Nolan, S. P. Flexible cycloalkyl-substituted N-heterocyclic carbenes. *Dalton Trans*. **2010**, *39*, 3923–3930; (c) Fortman, G. C.; Scott, N. M.; Linden, A.; Stevens, E. D.; Dorta, R.; Nolan, S. P. Unusual reactivities of N-heterocyclic carbenes upon coordination to the platinum(II)–dimethyl moiety. *Chem. Commun*. **2010**, *46*, 1050–1052.

(22) See the Supporting Information for further details.

(23) Zhang, Y.; Blacque, O.; Venkatesan, K. Highly Efficient Deep-Blue Emitters Based on cis and trans N-Heterocyclic Carbene Pt^{II} Acetylide Complexes: Synthesis, Photophysical Properties, and Mechanistic Studies. *Chem. Eur. J*. **2013**, *19*, 15689–15701 and references therein.

(24) (a) Campos, J.; Ortega-Moreno, L.; Conejero, S.; Peloso, R.; López-Serrano, J.; Maya, C.; Carmona, E. Reactivity of Cationic Agostic and Carbene Structures Derived from Platinum(II) Metallacycles. *Chem. Eur. J.* **2015**, *21*, 8883–8896; (b) Campos, J.; Peloso, R.; Carmona, E. Synthesis and Reactivity of a Cationic Platinum(II) Alkylidene Complex. *Angew. Chem. Int. Ed.* **2012**, *51*, 8255–8258.

(25) Baratta, W.; Stoccoro, S.; Doppiu, A.; Herdtweck, E.; Zucca, A.; Rigo, P. Novel T-Shaped 14-Electron Platinum(II) Complexes Stabilized by One Agostic Interaction. *Angew. Chem. Int. Ed.* **2003**, *42*, 105–108.

(26) Bassan R.; Bryars, K. H.; Judd, L.; Platt, A. W. G.; Pringle, P. G. Improved syntheses of [$PtMe_2$(1,5-COD)]. *Inorg. Chim. Acta* **1986**, *121*, L41–L42.

(27) Brookhart, M.; Grant, B.; Volpe, A. F. A $[(3,5\text{-}(CF_3)_2C_6H_3)_4B]^-[H(OEt_2)_2]^+$: Convenient Reagent for Generation and Stabilization of Cationic, Highly Electrophilic Organometallic Complexes. *Organometallics* **1992**, *11*, 3920–3922.

(28) CrysAlisPro RED, version 1.171.38.46: Oxford Diffraction Ltd., Oxford, U.K., 2015.

(29) SIR-97: Altomare, A.; Burla, M. C.; Camalli, M.; Cascarano, G.; Giacovazzo, C.; Guagliardi, A.; Moliterni, A. G. C.; Polidori, G.; Spagna, R. *J. SIR*97: a new tool for crystal structure determination and refinement. *Appl. Crystallogr.* **1999**, *32*, 115–119.

(30) SHELXL-2014: Sheldrick, G. M. A short history of *SHELX*. *Acta Crystallogr., Sect. A: Found. Crystallogr.* **2008**, *64*, 112–122.

(31) WINGX, version 2013.3: Farrugia, L. J. *WinGX* and *ORTEP for Windows*: an update. *J. Appl. Crystallogr.* **2012**, *45*, 849–854.

(32) MERCURY, CSD 3.9 (build RC1): Cambridge Crystallographic Data Centre, Cambridge, U.K., 2016.

(33) Chai, J.-D.; Head-Gordon, M. Long-range corrected hybrid density functionals with damped atom-atom dispersion corrections. *Phys. Chem. Chem. Phys.* **2008**, *10*, 6615–6620.

(34) (a) Ehrlich, S.; Moellmann, J.; Grimme, S. Dispersion-Corrected Density Functional Theory for Aromatic Interactions in Complex Systems. *Acc. Chem. Res.* **2013**, *46*, 916–926. (b) Grimme, S. Density functional theory with London dispersion corrections. *Comp. Mol. Sci.* **2011**, *1*, 211–228. (c) Schwabe, T.; Grimme, S. Theoretical Thermodynamics for Large Molecules: Walking the Thin Line between Accuracy and Computational Cost. *Acc. Chem. Res.* **2008**, *41*, 569–579.

(35) Figgen, D.; Peterson, K. A.; Dolg, M.; Stoll, H. Energy-consistent pseudopotentials and correlation consistent basis sets for the 5*d* elements Hf–Pt. *J. Chem. Phys.* **2009**, *130*, 164108–164120.

(36) Dunning, T. H. Gaussian basis sets for use in correlated molecular calculations. I. The atoms boron through neon and hydrogen. *J. Chem. Phys.* **1989**, *90*, 1007–1023.

(37) (a) Barone, V.; Cossi, M. Quantum Calculation of Molecular Energies and Energy Gradients in Solution by a Conductor Solvent Model. *J. Phys. Chem. A* **1998**, *102*, 1995–2001. (b) Cossi, M.; Rega, N.; Scalmani, G.; Barone, V. Energies, structures, and electronic properties of molecules in solution with the C-PCM solvation model. *J. Comput. Chem.* **2003**, *24*, 669–681.

(38) Frisch, M. J.; Trucks, G. W.; Schlegel, H. B.; Scuseria, G. E.; Robb, M. A.; Cheeseman, J. R.; Scalmani, G.; Barone, V.; Mennucci, B.; Petersson, G. A.; Nakatsuji, H.; Caricato, M.; Li, X.; Hratchian, H. P.; Izmaylov, A. F.; Bloino, J.; Zheng, G.; Sonnenberg, J. L.; Hada, M.; Ehara, M.; Toyota, K.; Fukuda, R.; Hasegawa, J.; Ishida, M.; Nakajima, T.; Honda, Y.; Kitao, O.; Nakai, H.; Vreven, T.; Montgomery, J. A., Jr.; Peralta, J. E.; Ogliaro, F.; Bearpark, M.; Heyd, J. J.; Brothers, E.; Kudin, K. N.; Staroverov, V. N.; Kobayashi, R.; Normand, J.; Raghavachari, K.; Rendell, A.; Burant, J. C.; Iyengar, S. S.; Tomasi, J.; Cossi, M.; Rega, N.; Millam, J. M.; Klene, M.; Knox, J. E.; Cross, J. B.; Bakken, V.; Adamo, C.; Jaramillo, J.; Gomperts, R.; Stratmann, R. E.; Yazyev, O.; Austin, A. J.; Cammi, R.; Pomelli, C.; Ochterski, J. W.; Martin, R. L.; Morokuma, K.; Zakrzewski, V. G.; Voth, G. A.; Salvador, P.; Dannenberg, J. J.; Dapprich, S.; Daniels, A. D.; Farkas, O.; Foresman, J. B.; Ortiz, J. V.; Cioslowski, J.; Fox, D. J. *Gaussian 09*, revision A.01; Gaussian, Inc.: Wallingford, CT, **2009**.

Figure for the Abstract and Table of Contents